

# The involvement of three signal transduction pathways in botryllid ascidian astogeny, as revealed by expression patterns of representative genes

AMALIA ROSNER<sup>\*1</sup>, GILAD ALFASSI<sup>1,2</sup>, ELIZABETH MOISEEVA<sup>1</sup>, GUY PAZ<sup>1</sup>, CLAUDETTE RABINOWITZ<sup>1</sup>, ZIVA LAPIDOT<sup>1</sup>, JACOB DOUEK<sup>1</sup>, ABRAHAM HAIM<sup>2</sup> and BARUCH RINKEVICH<sup>1</sup>

<sup>1</sup>Israel Oceanographic and Limnological Research, National Institute of Oceanography, Haifa, Israel and <sup>2</sup>Department of Evolutionary & Environmental Biology, Faculty of Natural Sciences, University of Haifa, Mount Carmel, Haifa, Israel

**ABSTRACT** The patterning of the modular body plan in colonial organisms is termed astogeny, as distinct from ontogeny, the development of an individual organism from embryo to adult. Evolutionarily conserved signaling pathways suggest shared roots and common uses for both ontogeny and astogeny. Botryllid ascidians, a widely dispersed group of colonial tunicates, exhibit an intricate modular life form, in which astogeny develops as weekly, highly synchronized growth/death cycles termed blastogenesis, abiding by a strictly regulated plan. In these organisms both astogeny and ontogeny form similar body structures. Working on *Botryllus schlosseri*, and choosing a representative gene from each of three key Signal Transduction Pathways (STPs: Wnt/ $\beta$ -catenin; TGF- $\beta$ , MAPK/ERK), we explored and compared gene expression at different stages of ontogeny and blastogenesis. Protein expression was studied via immunohistochemistry, ELISA and Western blotting. Five specific inhibitors and an activator for the selected pathways were used and followed to assess their impact during the blastogenic cycle and the development of distinctive phenotypes. Outcomes show that STPs are activated and function (while not necessarily co-localized) during both ontogeny and astogeny. Cellular patterns in blastogenesis, such as colony architecture, are shaped by these STPs. These results are further supported by administering Wnt agonist and antagonist, TGF- $\beta$  receptor antagonists and inhibitors of Mek1/Mek2. Independent of their expression during ontogeny, some of the spatiotemporal patterns of STPs developed within short blastogenic windows. The results support the notion that while the same molecular machinery is functioning in *Botryllus schlosseri* astogeny and ontogeny, astogenic development is not an ontogenic replicate.

**KEY WORDS:** *Botryllus schlosseri*, blastogenesis, MAPK/ERK, TGF- $\beta$ , Wnt/ $\beta$ -catenin

## Introduction

In colonial organisms each genetic entity (genet) is composed of a few to innumerable genetically identical units (modules), which emerge by diverse forms of budding (often named 'asexual reproduction' processes) from a single sexually produced larva, the founder module. Colonial structures, a tessellation of their structural modules (Rinkevich, 2002), are shaped by repetitions of a single structural unit or by nested modularity. The process and pattern of forming a colony is distinct from ontogeny (the development of the founder module in a colonial organism, or of the organism, in the case of a unitary entity), and termed astogeny (Pachut *et al.*, 1991; Rinkevich, 2002; Sánchez and Lasker, 2003). Astogeny is

controlled by a combination of genetically mediated developmental programs and environmental cues (Rinkevich, 2002; Sánchez and Lasker, 2003), allowing the formation of species-specific architecture through integrated, fixed and variable developmental pathways (Rinkevich, 2002; Shaish *et al.*, 2007). The developmental homeostasis throughout astogeny, universally reflected by high fidelity in the setting of morphological structures (Pachut *et al.*, 1991; Rinkevich, 2002; Sánchez and Lasker, 2003; Hughes, 2005; Rosner *et al.*, 2006; Shaish *et al.*, 2007; Kuecken *et al.*, 2011), is presumably controlled by a network of gene expressions

*Abbreviations used in this paper:* CI, cell islands; mac-like, macrophage like; PGC, primordial germ cell; STP, signal transduction pathway.

\*Address correspondence to: Amalia Rosner. Israel Oceanographic and Limnological Research, National Institute of Oceanography, Tel Shikmona, P.O.Box 8030, Haifa 31080, Israel. Tel: +972-4-856-5233. Fax: 972-4-851-1911 e-mail: amalia@ocean.org.il

Accepted: 13 November 2014.

and transcription factors. Developing such a functioning network should involve a complex temporal and spatial interplay of molecular cascades and cellular, chemical and mechanical stimuli. Elucidating the operation of developmental genes that control distinct levels of ontogeny and astogeny is, therefore, of special interest (Rinkevich, 2002).

There are some more complex astogenic phenomena, such as those involving cycles of degeneration and regeneration of modules (parallel or sequentially operated). This mode of astogeny has been established as typical of many bryozoans, hydroids, compound ascidians and other taxa (Hughes, 2005), depicting a much more intricate modular life form, which surfaces even via the reiteration of identical colonial modules. One such example for astogeny is found in botryllid ascidians.

Botryllid ascidians are a small but widely distributed group of colonial stolidobranch tunicates, used commonly as a model system for the study of developmental biology. A typical colony of a botryllid ascidian consists of a few to several thousand morphologically and genetically identical, recurrently developed modular units, called blastozoids (also referred to as zooids; hierarchically arranged in three successive generations of structural modules; Fig.

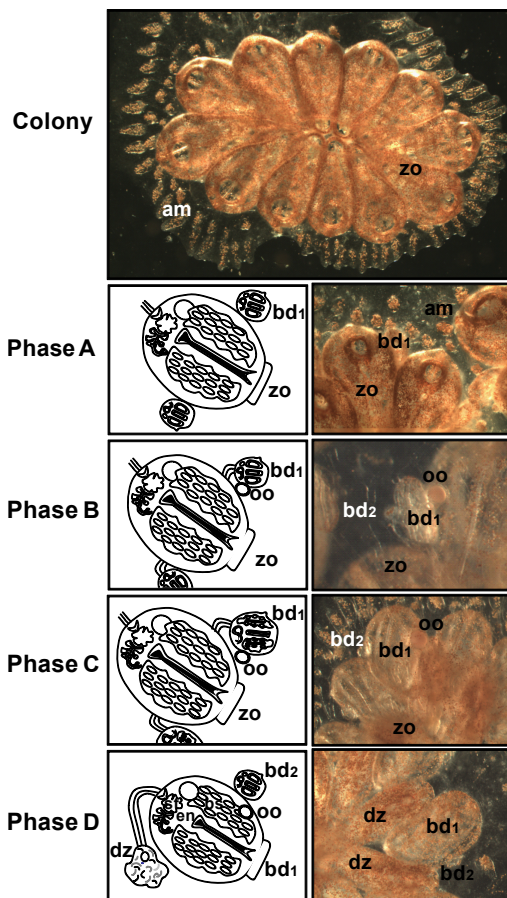


**Fig. 1.** *Botryllus schlosseri*. A typical colony of *Botryllus schlosseri* (upper panel) and the blastogenic phases “A” to “D” (sensu Mukai and Watanabe, 1976): schematic illustrations (left panels) of colonial phases (right panels). Abbreviations: am-ampulla; bd1-primary bud; bd2-secondary bud; bs-branchial sac; dz-degenerated zooid; en-endostyle; oo-oocyst; st-stomach; zo-zooid.

1). All zooids in a specific colony are encased within a common, translucent gelatinous tunic matrix and organized in elongated, compact, oval or star-shaped structures (systems) characteristic to each specific species. Zooids are connected to each other via a ramified vasculature, projecting along the colonial periphery in numerous sausage-like blind termini, the ampullae (Fig. 1). Although tightly interconnected morphologically and physiologically, each zooid within a colony is able to feed and sexually reproduce independently. In this group of organisms astogeny at 18-20°C develops as weekly, highly synchronized growth and death cycles, called blastogenesis, which adheres to a strictly regulated plan. The blastogenic cycle progresses simultaneously in all three co-existing, asexually derived generations; the functional zooids and the two successive cohorts of primary and secondary paleal buds (Berrill 1941a,b; Milkman 1967; Lauzon *et al.*, 2002; Manni *et al.*, 2007; Ballarin *et al.*, 2008). Each blastogenic cycle is composed of four major phases (Fig. 1), three of which display developmental processes (termed phases “A-C”; sensu Mukai and Watanabe, 1976), followed by a short fourth phase “D” (24 h period), a degenerative phase (also called ‘takeover’). During ‘takeover’ the old generation of zooids is eliminated through a whole-organismal apoptotic event ensued by swift phagocytosis (Cima and Ballarin, 2009), concurrently replaced by the primary buds that mature into the consecutive cohort of functional zooids (Fig. 1). Each blastogenic cycle, therefore, starts with the opening of the siphons of new adult zooids and ends in the takeover phase. During blastogenic phases “A” to “C”, as many as four new paleal buds may develop from the body wall of each functional zooid. Phase “A” primary buds (each may reach 0.3 mm long) carry the rudiments of the secondary buds that emerge from their atrial epithelium. Astogeny of the primary bud cohort precipitates during blastogenic phases “B” and “C” (reaching sizes of up to 1 mm), whereby the secondary buds concurrently form double-layered vesicles that initiate a rapid organogenesis process resulting in the formation of the primary buds of the next generation of colonial modules.

Botryllid ascidians are hermaphroditic species with male and female gonads situated side by side in each zooid. In the model species *Botryllus schlosseri*, ova mature in several consecutive blastogenic cycles during which they migrate to the developing buds of the succeeding generations (Sabbadin *et al.*, 1992), until ovulation and fertilization are finally attained with precise coordination between sexual reproduction and blastogenesis (Berrill, 1950; Milkman, 1967). Embryogenesis follows the blastogenic cycle, so that embryos held in the zooidal peribranchial chambers mature and hatch from the zooidal siphons just prior to blastogenic phase “D”, commencing zooidal regression and organ involution.

Detecting ontogeny within a colony requires separating the individual aspects of module growth from those of the founder module (oozooid, founder polyp, etc.). Therefore, when we look at the yet unknown cellular and molecular pathways, patterns, and rules which impose astogeny in colonial organisms, it is clear that elucidating the operation of astogeny associated developmental gene families is of fundamental interest, because the same gene families may have shaped ontogeny (e.g., Gasparini *et al.*, 2011). One of the preferred investigatory approaches utilizes Signal Transduction Pathways (STPs).

A STP is the process by which an extracellular signaling molecule activates a membrane receptor that in turn alters intracellular

**A1****Smad2**

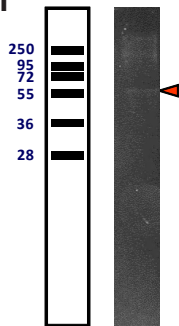
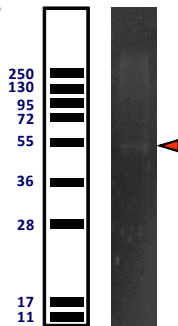
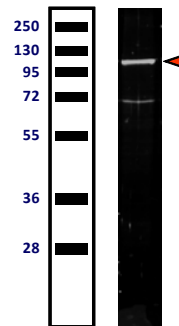
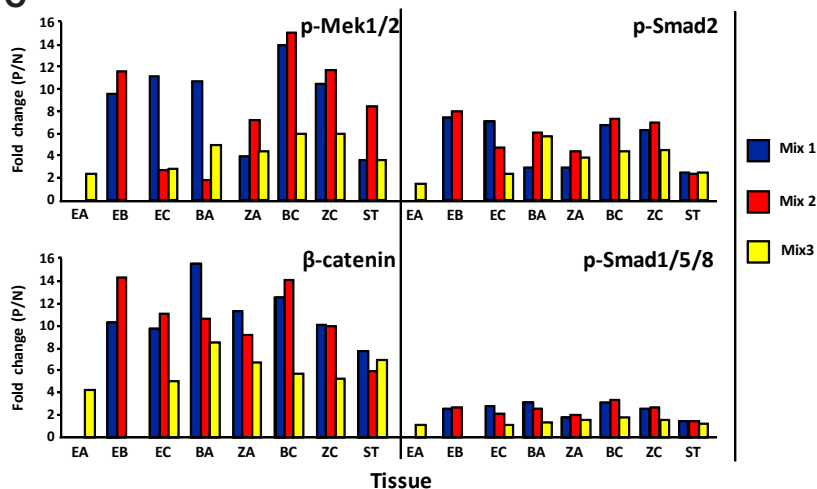
Human 249-**Q**SVN**Q**GFEAVYQLTRMCTIRMSFVKGWGAERYRQIVTSTPCWIELHLNGPLQWLDKVLTQMGS**PSIRCS**SVS-320  
*B. schlosseri* 603-**H**SVN**Q**GFEAVYQLTRMCTIRMSFVKGWGAERYRQIVTATPCWIELHLNGPLQWLDKVLTQMGS**SRTTCS**SMS-818  
 g63688

**A2****Mek1**

Human 114-**E**LQVL**H**ECN**S**PYIVGFYGFYSDGEISICMEHMDGGSLDQVLKKA**GRI**PEQ**I**LGKVSIAV-173  
 + + + + + + + + + +  
*B. schlosseri* 120-**E**LQIL**H**DC**K**SPFIVGFYGFYSDGEISICMENMDAGSLDQVVKRARRI**PEP**ILGKVSIAV-179  
 g28277  
 Human 174-**I**KGL**T**YLR**E**K**H**K**I**MHRDVKPSNILVNSRGEIKLCDFGVSGQLIDSMAN**S**FV**G**TR**S**YMS**P**E-233  
 ++ + \* \*  
*B. schlosseri* 180-**L**RGL**H**YLR**V**SH**N**I**I**HRDVKPSNILVNSRGEIKLCDFGVSGQLIDSMAN**S**FV**G**TR**S**YMS**P**E-239  
 g28277

**A3****β-catenin**

Human 658-**V**LR**F**RM**S**ED**K**PQ**D**Y**K**KRL**S**VEL**T**S**L**F**R**TE**P**MA**W**NE**T**AD**L**GL**D**IG**A**Q**E**PL**G**YR**Q**DD**P**SYR-717  
 + + + + + + + + + +  
*B. schlosseri* 1962-**A**L**I**RM**S**ED**K**SN**D**Y**K**KRL**S**ve**l**ss**s**l**I**R**D**D**G**Y**P**T**D**LM**G**SS**G**M**A**MD**G**YS**M**PL**sh**h**ss**vg**sv**h-21411  
 g28277  
 Human 718-**S**F**H**SG**G**Y**Q**D**A**L**G**M**D**P**M**ME**H**EM**G**GH**P**G**A**D**Y**P**V**D-**G**LP**D**LG**H**AQ**---**D**L**MD**G**LP**P**GD**S**N**Q**-**L**A**W**F**---**D**T**D**L**-781  
 + + + + + + + + + +  
*B. schlosseri* 2142-**ss**q**h**sg**Y**-----**P**P**Q**G**H**M**D**Y**G**H**Q**Y**G**A**P**M**D**Q**G**LP**D**LG**D**V**N**LD**V**F**M**Q**D**G**Q**G**P**P**D**-----**L**E**W**M**S**N**D**T**D**L-2318  
 g28277

**B1****B2****B3****C**

molecules, inducing a response. Some of the well-characterized STPs, such as Wnt pathways, are evolutionarily conserved signaling pathways that regulate multiple aspects of metazoan development. STPs are known to participate in ontogeny, and are specifically essential throughout development, from early cell divisions and axis specification to full organogenesis (Komiya and

**Fig. 2. Antibody validation.**

**(A1-A3).** Similarities between partial sequences from the human Smad2 **(A1)**, Mek1 **(A2)** and β-catenin **(A3)** and their *B. schlosseri* orthologues. Comparisons are between the sequences of the human assumed immunogens which served to elicit the antibodies used in this study (the manufacturers do not provide their exact sequence) and *B. schlosseri* orthologues. The human immunogens are derived from: Smad2 accession No. NP\_001138574.1; Mek accession No. NP\_002746.1; β-catenin accession No. NP\_001895.1; \* marks the putative phosphorylated serine; + marks similar amino acids. Blue letters signify identity or similarity; red letters signify differences. **(B1-B3)** Western blot results for *B. schlosseri* protein extracts hybridized with the following antibodies: **(B1)** p-Smad2; **(B2)** p-Mek1/2; **(B3)**

β-catenin. Red arrowheads point to the relevant band. **(C)** ELISA quantification of β-catenin, p-Smad2, p-Smad1/5/8, p-Mek1/2 proteins in *B. schlosseri* tissues: stomachs from adult zooids, young embryos (from colonies at blastogenic phases "A" and "B"), mature embryos (phase "C" colonies), young buds (phase "A" colonies), mature buds (phase "C" colony), and zooids from blastogenic phase "A" and blastogenic phase "C" colonies. P/N ratios: P is the value for OD absorbed by protein extract and treated with the particular antibody and N (negative) is the background OD (see material and methods). Abbreviations: BA, phase 'A' buds; BC, phase 'C' buds; EA, phase 'A' embryos; EB, phase 'B' embryos; EC, phase 'C' embryos; ST, stomach; ZA, phase 'A' zooids; ZC, phase 'C' zooids.

Habas 2008). STP networks have been studied in solitary ascidians in relation to development (Imai *et al.*, 2000; Nishida, 2003; Kourakis and Smith 2007). However, current knowledge on the signaling cascades in colonial ascidians is rudimentary, despite the common belief that the tunicates represent the closest living relatives of the vertebrates (Delsuc *et al.*, 2006). In fact, to-date only a few studies on STPs in colonial ascidians have been published (Franchi *et al.*, 2013; Kawamura *et al.*, 2013).

As the theorized networks of molecular pathways and mechanisms underlying *Botryllus schlosseri* astogeny are still unknown, we wish to examine the participation of a representative from three important STPs in colony blastogenesis (Wnt/β-catenin; Transforming Growth Factor Beta [TGF-β], Mitogen-Activated Protein Kinase [MAPK/ERK]). Examination of the *B. schlosseri* genome database (<http://genepyrmaid.stanford.edu/botryllusgenome/>) revealed the existence of the genes functioning in each of these pathways. As signals in these pathways are conveyed through post-translational modifications like phosphorylation, we chose

representative genes central to each of the above STPs, and looked for the specific spatio-temporal patterns of expression of the activated protein and the impacts of their modulation by specific agonist/inhibitors, thus laying the ground for future research.

## Results

### Identification of key molecules functioning in STPs

Verifying the functions of Wnt/ $\beta$ -catenin, MAPK/ERK and TGF- $\beta$  pathways in *B. schlosseri* blastogenesis requires the display of potential key molecules from each of these STPs. For this purpose, the *B. schlosseri* DNA whole genome database (Voskoboynik et al., 2013; <http://genepyrmaid.stanford.edu/botryllusgenome/>) was searched for the orthologues of genes functioning in each of these pathways. The results (Table 1) revealed the existence of at least one orthologue for each of the central families of proteins (ligands, receptors or second messengers), essential for successful signal transduction within each of the pathways: Wnt/ $\beta$ -catenin, MAPK/ERK and TGF- $\beta$ .

### General quantification of signal transduction pathways in *B. schlosseri*

Signal transduction during ontogenesis and blastogenesis in *B. schlosseri* colonies was monitored with commercial antibodies for activated effectors functioning in each pathway. Distributions of the phosphorylated forms of Smad2 (p-Smad2) and Smad1/5/8 (p-Smad1/5/8) were used to validate TGF- $\beta$  superfamily signaling, nuclear  $\beta$ -catenin for canonical Wnt pathway activation and phosphorylated form of Mek1/2 (p-Mek1/2) proteins for MAPK/ERK activation. Commercial anti Smad1/5/8 antibodies have already been proven to cross-react with *B. schlosseri* orthologues (Rosner et al., 2013). The previously undetermined specificities of the other antibodies were resolved in this study; We've shown a high sequence similarity between putative human derived immunogens (the exact sequences are not provided by the manufacturers), which served to elicit antibodies for each of the antigens p-Smad2, p-Mek1/2 or  $\beta$ -catenin and corresponding *B. schlosseri* orthologues (Fig. 2 A1-A3). The phosphorylation sites of the *B. schlosseri* orthologues of Smad2 and Mek1/2 were preserved. Western blot analyses revealed bands at size ranges similar to those observed in human (p-Smad2 52-56kDa; p-Mek1/2 43kDa;  $\beta$ -catenin 95kDa; Fig. 2 B1-B3). The western blot analysis with  $\beta$ -catenin revealed, in addition to the expected band, a second band of about 70kDa which might be a proteolytic cleaved fragment of  $\beta$ -catenin, as described previously in other animal models (Steinhusen et al., 2000; Fig. 2B3).

Using ELISA (Fig. 2C), the relative quantity of each one of the proteins ( $\beta$ -catenin, p-Smad2, p-Smad1/5/8, and p-Mek1/2) was measured in young embryos (at blastogenic phase "A"), embryos at an early tailbud stage (blastogenic phase "B"), mature embryos (at blastogenic phase "C"), buds at blastogenic phases "A" and "C" (each sample included primary and secondary buds of the respective phase), their corresponding blastogenic phases "A" and "C" zooids, and the digestive systems (stomachs and intestines) from blastogenic phase "A" colonies. The experiment was repeated three times. For each replicate the different proteins were extracted from 2-3 genets (referred to as 'Mix' in Fig. 2C). The results revealed common trends manifested through expression differences between buds and zooids and between colonies at different phases of the blastogenic cycle, while embryonic expressions fluctuated during

TABLE 1

### WNT/ $\beta$ CATENIN, MAPK/ERK AND TGF- $\beta$ PATHWAYS-SIGNALING MOLECULES AND THEIR SECOND MESSENGERS

Pathway	Genes		
	Gene family	Human	<i>Botryllus schlosseri</i> orthologues
Wnt/ $\beta$ catenin	Ligand-Wnt	wnt1	g54946
		Wnt2	g47754
		Wnt 2b	g27946
		wnt4a	g26693
		wnt4	g30622
		wnt5a	g37572
		wnt5b	g13032 and g39640
		wnt6	g6835
		wnt7a	g46011
		wnt7b	g34723
		wnt9a	g46318 and g46409
	Wnt16	g65512	
	Receptor -Frizzled	Fzd6	g46517
		Fzd8	g46146
Fzd9		g2573	
Fzd10B		g40914	
Co-Receptor-LRP-5/6	LRP6	g29158 and g71979 and g29600	
Disheveled	DVL1	g4586	
	DVL2 or DVL3	g58894	
Axin	Axin	g15404 and g39628	
Gsk3	Gsk3B	g4932 and g42386	
	Gsk3A	g4933	
$\beta$ -catenin	Ctnnb1	g33590 or g37700	
APC	APC2	g28914	
Ck1 $\alpha$	CSNK1A1	g67692 or g63618 or g68308 or g68309	
Ck1 $\gamma$	CSNK1G-1	g8766	
	CSNK1G2	g29328	
TCF/LEF	Cs-tcf	botctg013995	
MAPK	Ligand-FGF	fibroblast growth factor 4/5/6 ( <i>ciona intestinalis</i> )	g66473
	Receptor-FGFR	FGF1	g388
		FGF2	g16802
		FGF3	g43697
	GRB2	GRB2	botctg116393
	SOS	SOS1	g65732 and g65733
		SOS2	g33342
	RAS	Ras homologue	Contig3579
	RAF	Raf	Bot_oas_12269
	MEK	MEK1	g28277
	ERK (MAPK)	Mapk	g15151
	MKNK	MKNK1	g4411
	CREB	Creb1	g1780
	RSK	RPS6KB1	g1716 and g48067 and g31986
RPS6KD1		g3273 and g5202 and g12504 and g12506	
RPS6KA5		g562 and g11760 and g36058 and g11761	
MYC	Myc	g41847	
TGF- $\beta$	TGF $\beta$ ligands	BMP 2/4	g31245 and g47032
		BMP3	g8422
		Nodal	g61407 and g69207
		TGF $\beta$	g70350
	Type II receptors	activin A receptor type II- ACVR2A	g24835
		TGF $\beta$ RII	g37571
	Type I receptors	activin A receptor type IB - ACVR1B	g28159
		TGF $\beta$ RI	g10147
	zinc double finger FYVE domain containing protein	Hrs1	g65576
	R-SMAD	Smad1	g27283
		Smad1/5	g20069
		Smad2/3	g8970 or g62108 or g63688
	coSMAD	Smad4	g55480 or g63821

Human and the *B. schlosseri* orthologues are shown. 'g' stands for gene.

differentiation:  $\beta$ -catenin quantity was always higher in buds than in zooids, with relatively high quantities also found in embryos; p-Smad2 highest expression was detected during the embryonic tailbud stage. In the colony, p-Smad2 expressions in buds and zooids of phase 'C' were higher than in phase 'A' appropriate tissues; p-Mek expressions were the highest in buds of phase 'C'; finally the expressions of p-Smad1/5/8 were relatively low, with a slightly higher expression in buds than in zooids.

To further study the typical expression patterns of these proteins in normal colonies, *B. schlosseri* genotypes were subcloned, each into four ramets, sacrificed in blastogenic phases "A" to "D" and prepared for immunohistochemistry. Using histological sections of whole gravid ramets enabled the study blastogenesis of in *B. schlosseri* colonies, simultaneously to major stages of ontogeny (expressions of the signal transductions genes in developed gonads and in embryos). The results are shown henceforth.

### The Wnt pathway

#### Normal expression during blastogenesis and embryogenesis

$\beta$ -catenin expression patterns in ontogeny and blastogenesis were studied, with emphasis on  $\beta$ -catenin accumulation in cell nuclei (Fig. 3 A-X). Examination of mature oocytes (Fig. 3A) through embryogenesis (Fig. 3 B-H) up to the late embryo (Fig. 3 I-K) revealed nuclear accumulation of  $\beta$ -catenin in two main developmental stages: at vegetal poles in early embryos (Fig. 3B), similarly to other ascidians (Hudson *et al.*, 2013), and in the endostyles (endodermal origin) of late embryos (Fig. 3I-K). Otherwise, expressions were low and homogeneous in nuclei and cytoplasm during embryogenesis. By comparison, the strong expression of  $\beta$ -catenin at cell periphery, probably as part of the adherens junctions (Oda, 2012), became evident from gastrulation (Fig. 3C) and intensified during the later stages of embryo differentiation (Fig. 3 D-K).

Along blastogenesis, the differentiating buds (Fig. 3 L-P) revealed a weak but homogenous  $\beta$ -catenin distribution in the cytoplasm and nuclei and high expressions at cell boundaries, from the crescent-like stage of secondary buds (Fig. 3L) to the fully differentiated primary buds at the end of blastogenic phase "D". Prominent nuclear expressions were not detected during bud differentiation, including in the endostyles. In most zooidal tissues, we did not detect accumulated  $\beta$ -catenin nuclear staining, but rather weak homogenous staining in cytoplasm and nuclei and strong staining at cell boundaries (Fig. 3 Q-S). Cells in the cell island (CI) compartments along the endostyle were the only tissues with prominent nuclear staining in mature zooids (Fig. 3T). Zone 4 in the zooidal endostyle (Fig. 3U) was the most intensively stained tissue during phases A-C (Fig. 3V). At late blastogenic phase "C", a change occurred as cells from the endostyle zone 4 and some loose cells in close proximity were completely deprived of nuclear  $\beta$ -catenin stain (Fig. 3W). Peripheral  $\beta$ -catenin staining persisted at the beginning and middle blastogenic phase "D" (Fig. 3X) and the 'takeover' phase (Mukai and Watanabe, 1976; Cima and Bal-larin, 2009).

In the germ lineage, cytoplasmic and nuclear expressions were detected in the PGC-like (primordial germ cells; Rosner *et al.*, 2013) or gonial cells (Fig. 3P). In differentiating germ cells within the buds, the expression was weak and restricted to the periphery of the oocytes (Fig. 3L) or the male cells (Fig. 3P).  $\beta$ -catenin expressions were not detected in mature zooidal testes.

#### Impact of Wnt agonist and antagonist

The Wnt agonist (WA; 2-Amino-4-(3,4-(methylenedioxy) benzylamino)-6-(3-methoxyphenyl) pyrimidine; Liu *et al.*, 2005) was employed at a concentration of 0.05  $\mu$ M, and distinctive phenotypes were recorded for 4-21 days following drug administration. Preliminary studies revealed that concentrations >0.1  $\mu$ M caused

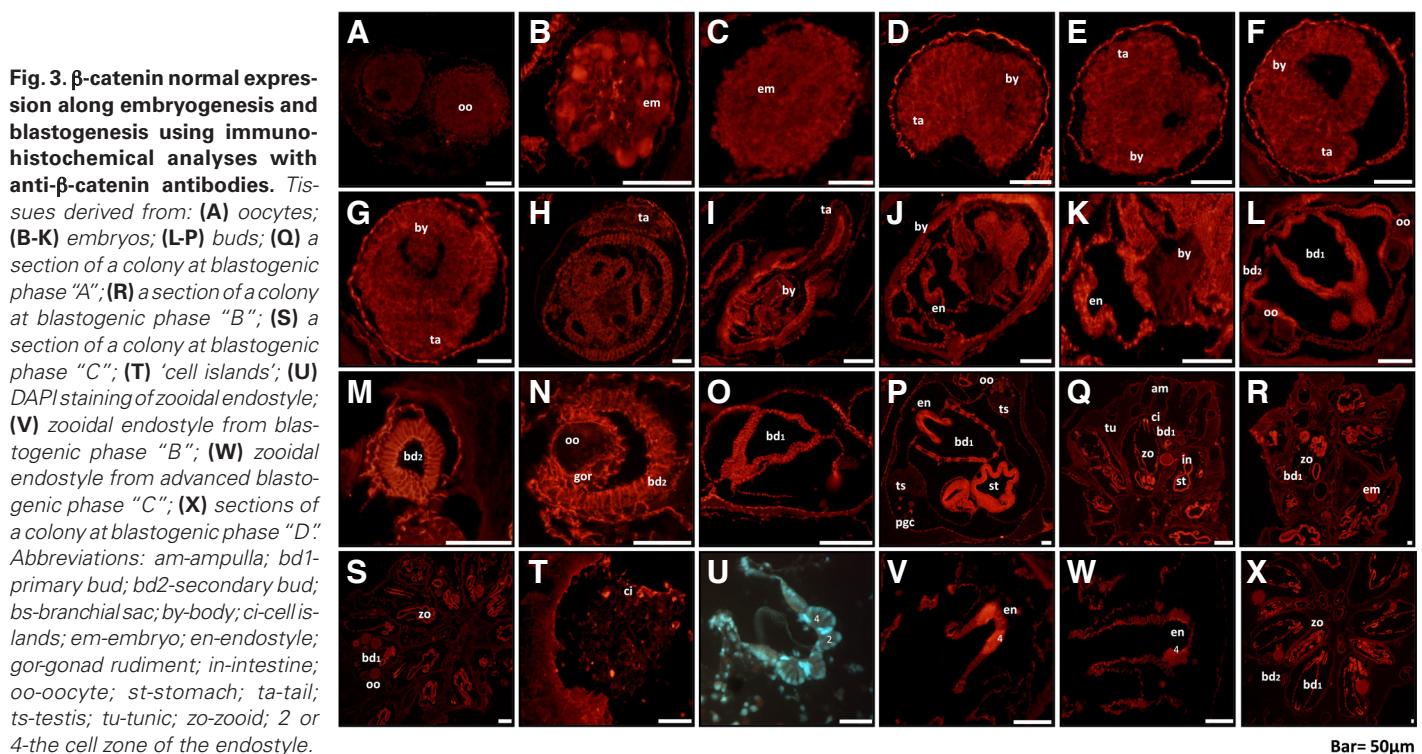


**Fig. 3.  $\beta$ -catenin normal expression along embryogenesis and blastogenesis using immunohistochemical analyses with anti- $\beta$ -catenin antibodies.** Tissues derived from: (A) oocytes; (B-K) embryos; (L-P) buds; (Q) a section of a colony at blastogenic phase "A"; (R) a section of a colony at blastogenic phase "B"; (S) a section of a colony at blastogenic phase "C"; (T) 'cell islands'; (U) DAPI staining of zooidal endostyle; (V) zooidal endostyle from blastogenic phase "B"; (W) zooidal endostyle from advanced blastogenic phase "C"; (X) sections of a colony at blastogenic phase "D." Abbreviations: am-ampulla; bd1-primary bud; bd2-secondary bud; bs-branchial sac; by-body; ci-cell islands; em-embryo; en-endostyle; gor-gonad rudiment; in-intestine; oo-oocyte; st-stomach; ta-tail; ts-testis; tu-tunic; zo-zooid; 2 or 4-the cell zone of the endostyle.

Bar= 50 $\mu$ m

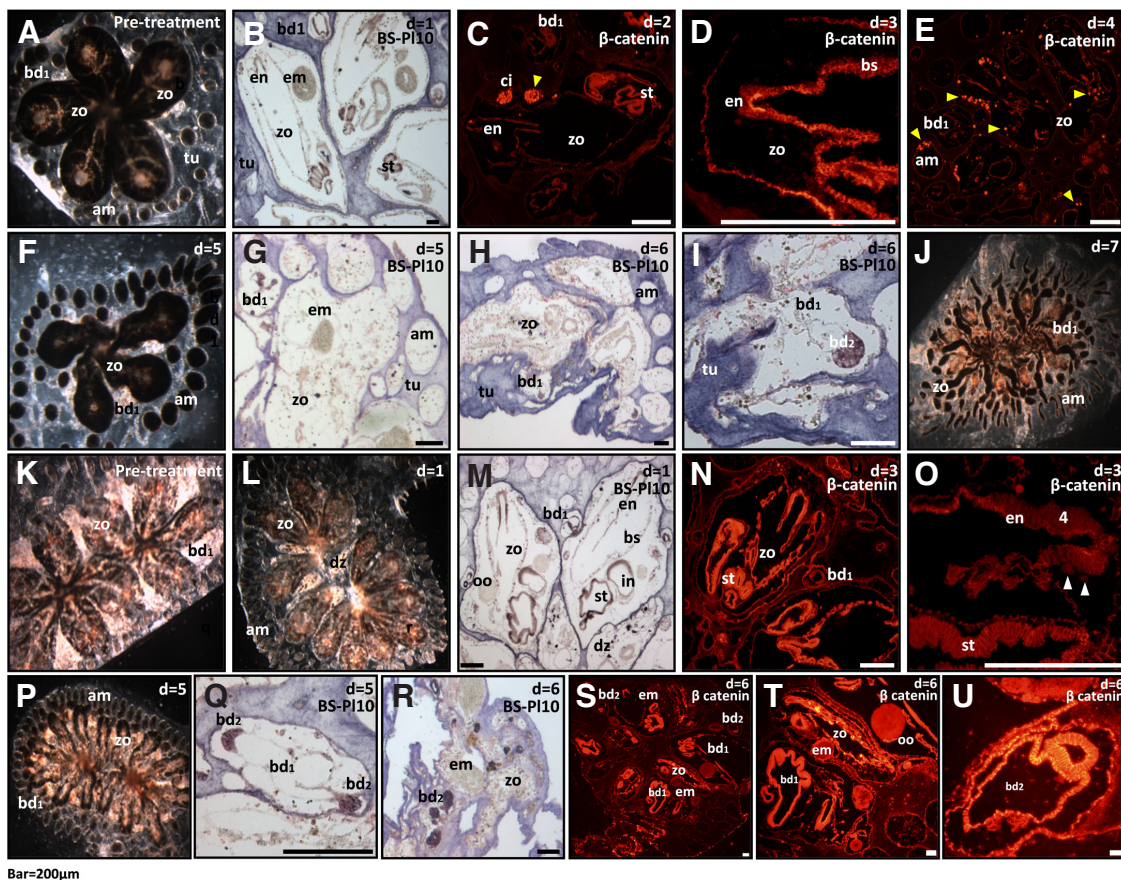


**Fig. 4. Deregulation of Wnt pathway by altering  $\beta$ -catenin levels in *B. schlosseri* colonies.** *Wnt* agonist (**B-R**) and *Wnt* antagonist (**S-U**) impacts; gross morphologies of *B. schlosseri* colonies (**A,F,J-L,P**), and immunohistochemical analyses (**B-E,G-I,M-O,Q-U**) performed with either  $\beta$ -catenin or BS-PL10, as specified for each sub-figure. Immunohistochemical signals were visualized with alkaline phosphatase (AP) conjugated secondary antibodies (**B,G-I,M,Q-R**), or with cy3-conjugated antibodies (**C-E,N-O,S-U**). Each sub-figure specifies time from onset *Wnt* agonist/antagonist administration ( $d=0$ ). The panels include: (**A**) phase "A" colony before treatment ( $d=0$ ); (**B-J**) phase "A" colonies treated with *Wnt* agonist at various time points; (**K**) phase "C" colony before treatment; (**L-R**)

phase "C" colonies treated with *Wnt* agonist at various time points; (**S-U**) sections from colonies treated with *Wnt* antagonist. Yellow arrowheads point to macrophage-like cells; white arrowheads point to cells without  $\beta$ -catenin nuclear staining. Abbreviations: am, ampulla; bd1, primary bud; bd2, secondary bud; bs, branchial sac; ci, cell islands; dz, degenerated zoid; em, embryo; en, endostyle; in, intestine; oo, oocyte; st, stomach; tu, tunic; zo, zoid.

colonial mortality, whereas concentrations of  $<0.01 \mu\text{M}$  had no phenotypic outcomes (data not shown). In total, 16 colonies at blastogenic phases "A" and "B" (13 experimental, 3 controls) and 7 colonies at late phases "C" and "D" (5 experimental, 2 control) were treated for 24 h with WA (agonist first incubation day assigned as day 0) and closely monitored for up to 21 days thereafter (Fig. 4). Treatment impacts were evaluated by observing the colonies under binocular stereomicroscopy or by immunohistochemical analyses with  $\beta$ -catenin or BS-PL10 antibodies (Rosner et al., 2006). BS-PL10 expression differentiated between bud tissues (high expression) and zooidal tissues (low expressions; Rosner et al., 2006). On day 1 following treatment ( $d=1$ ), all colonies looked similar to controls (Fig. 4A) and the functional zooids exhibited normal heart pulsations and blood cell circulation. Immunohistochemical analyses confirmed the integrity of colonial morphologies (Fig. 4B). Thereafter, the documented responses were associated with the blastogenic phase of the colony when subjected to *Wnt* agonist; on day 2, cell islands (CI) of zooids treated at the beginning of the blastogenic cycle (phases "A" or "B") were populated by aggregates of macrophage-like (mac-like) cells with high  $\beta$ -catenin expression (Fig. 4C, yellow arrow). On day 3, signs of stress manifested by blood vessels dilatation and accumulation of cells in blood vessels were documented. Additionally, the integrity of the internal organs of buds and zooids were affected, as tissues became thinner and expression of  $\beta$ -catenin decreased in tissues where they are

normally elevated, as in the zooidal endostyle zone 4 (Fig. 4D). On day 4, simultaneously with the appearance of morphological degradation, dispersed  $\beta$ -catenin heavily-stained mac-like cells were unexpectedly spotted outside of CI in early phase "C" zooids and ampullae (Fig. 4E, yellow arrows), a phenomenon normally occurring in blastogenic phase D colonies. In these colonies, buds' tissues were underdeveloped, although not populated with mac-like cells (Fig. 3E). On day 5 buds were smaller than expected from their chronological age. Zooids shrank and rotated relative to each other within the system, thus failing to form common exhalant siphons (Fig. 4F). Blood cells, typically traced through circulation of distinguished cell types like pigment cells, moved into the ampullae, which were transformed into dilated structures, up to four times larger than normal. Immunohistochemical analysis further revealed complete destruction of embryos and zooidal internal organs as well as degenerated bud tissues (Fig. 4G). These deformed bud tissues expressed high levels of BS-PL10 as do normal buds (Rosner et al., 2006). On day 6, the only 'healthy looking' tissues were the crescent-like BS-PL10 positive undifferentiated epithelial-like tissues, which resembled early differentiating secondary buds (Fig. 4H,I). Thereafter, while control colonies started a new blastogenic cycle, the zooids of the treated colonies shrank to a minimum but were not absorbed at the end of the blastogenic cycle (Fig. 4J). In most cases the colonies continued to deteriorate until blood movement ceased and the colonies died. In a few cases, after a

prolonged and unusual blastogenic cycle of the treated zooids (>9 days), a few buds managed to endure the ‘takeover’ phase and started a new blastogenic cycle.

When colonies at late blastogenic phase ‘C’ (Fig. 4K) to early phase ‘D’ were treated with Wnt agonist, the first blastogenic cycle progressed contemporaneously as the control colonies, developing morphologically normal zooids (Fig. 4L), a result which was further supported by an immunohistochemical analysis with BS-PL10 antibody (Fig. 4M). Following three days of treatment, the newly formed primary buds were morphologically underdeveloped compared to the controls, although zooidal internal organs seemed normal (Fig. 4N). Thorough immunohistochemical examinations revealed an abnormal status, as cells with no nuclear  $\beta$ -catenin staining were documented in zooidal endostyle zone 4 and in its proximity (Fig. 3O, white arrow), similar to the mode of expression in late phase ‘C’ normal colonies (Fig. 3W). On day 5, a deteriorating colony phenotype developed (Fig. 4P). Immunological analyses with BS-PL10 antibodies revealed zooidal and primary buds destruction (Fig. 4Q), concomitantly with developing BS-PL10<sup>+</sup> crescent-like shaped secondary buds (Fig. 4Q) that appeared similar to those

observed in colonies treated at blastogenic phase ‘A’ (Fig. 4H,I). On day 6, the secondary buds were at an early differentiation state (Fig. 4R). In one case, three early differentiating buds were detected within a single common epithelial envelope, each of which differentiated along its own longitudinal axis (Fig. 4R). On day 7, while the control colonies entered into the ‘takeover’ phase and proceeded to the new blastogenic cycle, the treated colonies remained in a prolonged blastogenic ‘D’ phase for two additional days. By day 21, zooidal systems in some of the treated colonies had completely recovered. Altogether, only 3 out of 13 (23%) colonies from blastogenic phases ‘A / B’ and 3 out of 5 (60%) colonies from phase ‘C’ survived treatment.

Further deregulation of the Wnt pathway in *B. schlosseri* colonies was achieved using the Wnt antagonist XAV939, an inhibitor of Tankyrase (IC<sub>50</sub>=4nM; The *B. schlosseri* orthologue of Tankyrase in the genome database is g65078). Seven naïve colonies were exposed to 4nM XAV939 for three days before being transferred to normal sea water. Following treatment, we observed short blastogenic cycles (lasting five or six days) in five of the treated colonies (71%). In three colonies, we detected abnormalities in

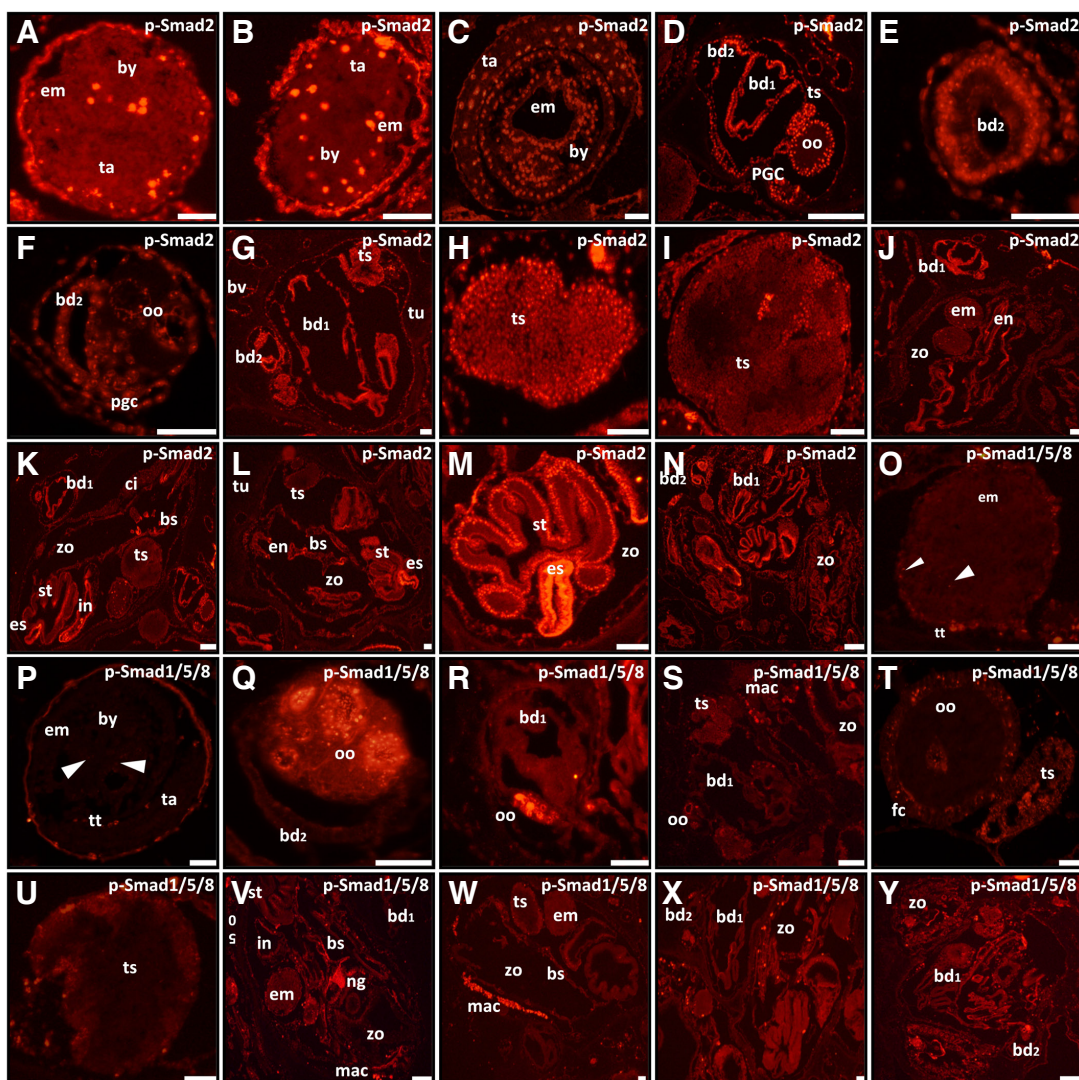


**Fig. 5. p-Smad2 and p-Smad1/5/8 normal expressions along embryogenesis and blastogenesis. (A-N)** Immunohistochemical analyses of various *B. schlosseri* tissues with anti p-Smad2 antibodies. The examined tissues are: (A-C) embryos; (D-G) buds; (H) testis from primary bud; (I) zooidal testis; (J) blastogenic phase ‘A’ colony; (K) blastogenic phase ‘B’ colony; (L) blastogenic phase ‘C’ colony; (M) zooidal esophagus and stomach; (N) blastogenic phase ‘D’ colony; (O-Y) immunological analyses of various *B. schlosseri* tissues with anti p-Smad1/5/8 antibodies. The examined tissues are: (O-P) embryos; (Q-S) buds; (T) oocyte and testis from a primary bud; (U) zooidal testis; (V) blastogenic phase ‘A’ colony; (W) blastogenic phase ‘B’ colony; (X) blastogenic phase ‘C’ colony; (Y) blastogenic phase ‘D’ colony. White arrows point to faint p-Smad1/5/8<sup>+</sup> staining in the embryos. Abbreviations: bd1, primary bud; bd2, secondary bud; bs, branchial sac; bv, blood vessel; by, body; ci, cell islands; em, embryo; en, endostyle; es, esophagus; fc, follicular cells; mac, macrophage-like cells; in, intestine; ng, neural gland; oo, oocyte; PGC, PGC-like cells; st, stomach; sy, syphon; ta, tail; ts, testis; tt, test cells; tu, tunic; zo, zooid.

Bar=50 $\mu$ m

embryo differentiation and in secondary buds (Fig. 4 S-U). In the treated colonies, dead or undifferentiated embryos were spotted in blastogenic phase 'D' zooids (Fig. 4 S-T). Simultaneously, several secondary buds with partially degenerated tissues were identified; however, this phenotype was not accompanied by a prominent decrease of  $\beta$ -catenin in the nuclei (Fig. 4U).

The overall impacts of Wnt agonist/antagonist administrations can be categorized into three main results: (1) changes related to the duration of the blastogenic cycle, prolonged by the agonist (affecting the absorption time of the old generation of zooids), while the antagonist caused cycle acceleration; (2) attenuation/arrest of bud differentiation, where the  $\beta$ -catenin agonist had impacts mainly on primary buds and the antagonist on the secondary buds; (3) the death of embryos, observed following both treatments.

### The TGF $\beta$ pathway

#### Recurrent expression

The TGF $\beta$  superfamily of ligands is divided into several sub-families whose signals are transduced by either Smad2/Smad3 or Smad1/Smad5/Smad8 pathways. Smad2 is a transcriptional modulator phosphorylated upon activation with TGF- $\beta$  or activin type 1 signals. This phosphorylation enables p-Smad2 association with Smad4 and their translocation into the nucleus where p-Smad2 exerts its function. In the *Botryllus* system, nuclear p-Smad2 staining increased gradually along embryogenesis (Fig. 5 A-C). Starting from nuclear staining of a few cells (Fig. 5A), the number of stained cells notably increased, showing temporal and spatial specificity with most of the staining being concentrated in the body tissue and not in the tail rudiment (Fig. 5B). At the wrapped-tail stage, nuclear p-Smad2 staining was detected in most embryonic cells (Fig. 5C). Bud staining showed different expression dynamics; nuclear p-Smad2 staining appeared in most soma bud cells from the moment new secondary buds developed in crescent forms (Fig. 5D). This staining continued through all bud stages (Figs. 5 D-G). Early differentiating oocytes (Fig. 5F) also expressed nuclear p-Smad2, whereas in mature eggs (Fig. 5D) expressions were detected only in the nuclei of the follicular and test cell layers, which wrap the eggs but without staining in the eggs. Positive staining was documented in the primordial germ cell-like cells (PGC-like; Rosner *et al.*, 2009; Fig. 5D) and bud testes (Figs. 5 G-H). The staining of the testes dropped dramatically in blastogenic phase "A" zooids to a few bundles of cells (Fig. 5I), and was absent from testes of blastogenic phase "C" zooids (Fig. 5L). Nuclear p-Smad2 staining was evident in zooidal soma tissues during phases "A-C", and extensively marked in the endostyles and in the digestive systems (Figs. 5 J-M). The zooidal esophagus exhibited a unique mode of staining, displaying the highest concentrations mainly in the cytoplasm (Fig. 5M). The zooidal staining decreased significantly as soon as the colonies entered blastogenic phase "D" (Fig. 5N).

P-Smad1/5/8 is phosphorylated upon activation by BMP (Bone Morphogenetic Protein) type 1 receptor kinase. The p-Smad1/5/8 expression pattern has already been studied in *B. schlosseri* with emphasis on the germ lineage (Rosner *et al.*, 2013). In the present study, extremely faint staining with p-Smad1/5/8 was detected within the embryonic tissues (white arrows; Figs. 5 O-P). Since the test cells wrapping embryos of various ages showed a significantly stronger expression, the pattern for embryonic staining is not clear. While bud soma of various developmental stages were not stained

(Figs. 5 Q-S), high expressions were detected in the germ lineage, in nuclei of PGC-like cells, oocytes (Fig. 5Q) and mature eggs, including staining in the follicular layers that wrap the eggs (Fig. 5T). The expression of p-Smad1/5/8 in testes was detected in the buds (Figs. 5 S-T), whereas in zooidal testes it dropped off and vanished in mature sperm (Fig. 5U). Along blastogenesis phases "A" to "C" zooids did not show distinctive staining changes; PGC-like and mac-like cell populations and the neural glands were the only cells/tissues stained with p-Smad1/5/8 in these zooids (Figs. 5 V-X). Thus, the distribution of PGC-like and mac-like cell populations within various zooidal compartments had its mark on overall zooidal staining. These results corresponded with the ELISA outcomes; the tissue limited distribution of p-Smad1/5/8 was in accordance with the low quantities of the protein detected by ELISA assay, while high expression in early germ lineage (situated in the buds) explains the relative increase of p-Smad1/5/8 protein in buds. At blastogenesis phase "D", the zooidal neural gland remained stained until completely degraded and at the same time a significant increase of staining was detected in the digestive systems undergoing apoptosis (Fig. 5Y).

#### SB-431542 and LY2157299 administration; the impact of TGF- $\beta$ inhibitors

SB-431542 is an inhibitor of endogenous activin and TGF- $\beta$  signaling but has no effect on BMP signaling (Inman *et al.*, 2002). The inhibitor was employed at a concentration of 5  $\mu$ M, and the fates of treated colonies were recorded for 20 days following drug administration. Preliminary studies revealed that concentrations of >7  $\mu$ M caused colonial mortality, whereas concentrations of <1  $\mu$ M resulted in no phenotypic outcomes (data not shown). In total, 11 colonies (8 experimental, 3 controls) at blastogenic phases "A" or "B" (the phenotype and hematoxylin-eosin of the control colonies are shown on Figs. 6 A-B, respectively) were treated for 72 h, and closely monitored for up to 21 days thereafter (Fig. 6 C-M).

After three days of exposure to SB-431542, the colonies which were transferred to regular seawater preserved an almost normal phenotype, with normal sized buds compared to controls (Fig. 6C). Hematoxylin-eosin histological sections revealed the appearance of large cavities in the right-hand sides of primary buds, which pushed the soma tissues to the left (Fig. 6D, red arrows). On day 6, a decrease of nuclear p-Smad2 staining in primary and secondary buds (Fig. 6E) was detected, and the colonies exhibited stress signs, manifested by retraction of the zooids towards the periphery of the colony (Fig. 6F). On day 7, together with reduced p-Smad2 expressions in stomach cell nuclei and diminished expressions in esophagus (Fig. 6G), malformations within the primary buds were observed (Figs. 6 H-J). In some of these buds, the endostyle tips and the branchial sacs (situated at the anterior side of the bud) were deformed or degenerated, while the well-developed digestive systems (posterior side) were tilted to the right, perhaps by the enlarged cavities. Early staged embryos with decreased p-Smad2 staining (Fig. 6K) were detected. Eventually, a new blastogenic cycle started, but from that point onwards, the colonies started deteriorating (Figs. 6 L-M). The new generation of zooids were rotated within the tunic and failed to form normal zooidal systems (Fig. 6M). The zooids further bent and twisted, while the buds deteriorated and their number decreased. Most of the colonies (5/8 colonies, 62.5%) died within 20 days. In the other three colonies, the few remaining stressed zooids regenerated through a series of abnormal zooidal generations ('striving for normality' sensu Voskoboynik *et al.*, 2007),

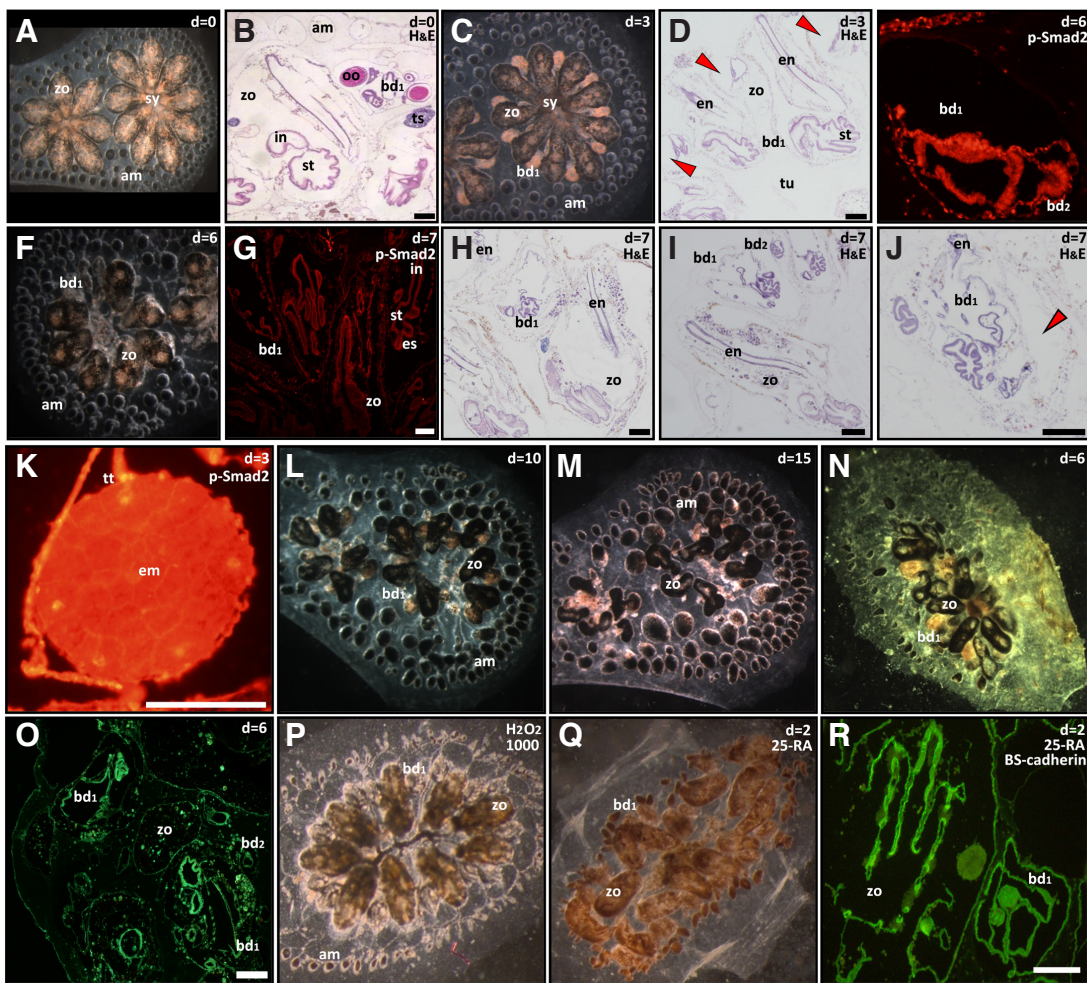


**Fig. 6. Documenting SB-431542 and LY2157299 impacts on *B. schlosseri* colonies.** Gross morphologies of *B. schlosseri* colonies (A, C, F, L-N, P-Q), hematoxylin and eosin staining (B, D, H-J), unspecific fluorescent emission from fixed section (O) and immunohistochemical analyses performed with either p-Smad2 (E, G, K) or BS-cadherin (R). Time after antagonist administration is specified, setting first treatment day as d=0. Panels include: (A-B) naïve colonies; (C-D) colonies subjected to SB-431542 for 3 days; (E-M) colonies recovering SB-431542 treatment in sea water; (N-O) colonies recovering LY2157299 treatment in sea water; (P) a colony after overnight submersion in 1000  $\mu\text{M}$   $\text{H}_2\text{O}_2$ ; (Q-R) colonies after overnight submersion in 25 nM retinoic acid. Red arrows point to abnormal cavities in primary buds. Abbreviations: am, ampulla; bd1, primary bud; bd2, secondary bud; bs, branchial sac; en, endostyle; es, esophagus; H&E, hematoxylin and eosin staining; in, intestine; oo, oocyte; st, stomach; sy, syphon; ts, testis; tu, tunic; zo, zooid.

a process that led to the development of rehabilitated colonies, presenting typical zooids and regular blastogenic cycles.

Naïve colonies were treated with another inhibitor of TGF- $\beta$  receptor type 1 kinase, LY2157299. *B. schlosseri* colonies were exposed to 30 nM ( $\text{IC}_{50}$ =56 nM) for three days. In 2/5 treated colonies the modules lost the system unit organization (Fig. 6N), and the stomach within some of the primary buds was pushed aside from its normal site (Fig. 6O). Embryos failed to differentiate, and some of the embryos were found trapped in stage D zooids. These results were in accordance with the impacts of SB-431542, suggesting that the effects of the antagonists are specific to the TGF- $\beta$  pathway.

Stress *per se*, such as oxidative stress (Fig. 6P), did not cause morphological changes as those observed after administration of the two antagonists. Rather, the antagonists induced changes resembling those caused by the administration of retinoic acid (Figs. 6 Q-R), a molecule known to determine the anterior-posterior axis of developing buds in *Polyandrocarpa misakiensis* (Hara *et al.*, 1992).

### The MAPK/ERK pathway

#### Recurrent expression

Here we studied expression patterns of p-Mek1/2, an enzyme which phosphorylates the mitogen-activated protein kinase (MAPK; Fig. 7). p-Mek1/2 expressions were detected in several cell compart-

ments: cytoplasm, nucleus and near the cell membrane (Fig. 7). In mature eggs p-Mek appeared as small aggregates spreading within the cytoplasm (Fig. 7A). Sporadic nuclear expression was detected in test cells and in the follicular layers wrapping the eggs. In early embryos the strongest expression was detected in the nuclei of a limited number of cells that form aggregates composed of 2-3 cells (Fig. 7B). Thereafter, staining in the form of small granules in the cytoplasm, in nuclei and in the form of continuous sub-membrane staining, appeared primarily in specific cell populations concentrated at one of the hemispheres of the embryos (Fig. 7C). At mid-tail stage, most embryonic tissues were stained, with differences in the subcellular location of the staining; granular staining appeared in the anterior part of the body while the sub-membranal and nuclear staining appeared in the posterior part of the body trunk. Strong staining of the epidermis lining the tip of the embryo tail and granular staining in the rest of the tail were also detected (Fig. 7D). In wrapped-tail embryos, all three subcellular staining distributions were detected, varying between the different tissues (Figs. 7 E,F). For example, in the tail of the embryo we detected a few stained cells scattered in the notochord and in the epidermis, at different sites along the tail. Secondary and primary buds also reflected three expression patterns: strong, whole cellular staining, staining of small cytoplasmic granules, and sub-membrane staining of cells at the apical side of the tissue (Fig. 7 G-K). In early secondary buds, tiny cytoplasmic

granular staining appeared starting from the crescent-like developmental stage (Fig. 7J). In parallel, a couple of whole-stained cells occasionally appeared in the soma tissues (Fig. 7 G-I). During blastogenesis, strong whole-cell staining increasingly appeared in a number of cells, predominantly in the primary bud cells of the gut and neural rudiments (Fig. 7J), and then, in the digestive system (Fig. 7K). In primary buds at blastogenic phase "C", apical-sided staining appeared in the endostyle (Fig. 7K) and gradually in other internal organs, until this apical sided staining pattern replaced the sporadic whole cell staining pattern. Apical sided staining of various zooidal internal organs persisted at blastogenic phases "A-C" (Figs. 7 L,M,O), and disappeared gradually with zooid absorption during blastogenic phase "D" (Fig. 7P). Counterstaining with DAPI confirmed that this apical side staining was not nuclear, since nuclei are situated basally within the tissue (Fig. 7N). A further follow up on p-Mek1/2 expression within the germ lineage revealed nuclear staining in young oocytes (Fig. 7J) which disappeared as they differentiated, remaining in the form of small cytoplasmic aggregates in the cytoplasm and the perinuclear region (Figs. 7 H-I). Strong whole-cell staining was detected in few cells within the gonad rudiment (Fig. 7G). The number of positively stained male cells increased but still marked only a fraction of the male cells in the bud testes (Fig. 7J). The zooidal testes at blastogenic phases "A" and "B" contained a few bundles of stained cells (Fig. 7L), which disappeared as testes matured during the blastogenic phase "C" (Fig. 7O). Finally, staining was detected in the cells situated in the tunic matrix, ampullae (Fig. 7O) and in some of the epithelial cells

lining the blood vessels (Fig. 7L).

Depending on its cellular context, MAPK/ERK pathway mediates diverse biological functions, including cell proliferation (Liu *et al.*, 2004). To test possible function of MAPK/ERK in cell proliferation, the p-Mek 1/2 expression pattern was compared to that of phosphorylated Histone3 (p-H3, the core protein of the nucleosome and a well-documented marker of cell proliferation; Figs. 7Q-T). The staining pattern of p-Histone3 (p-H3) overlapped the staining patterns of the whole/nuclear p-Mek1/2 stained cells.

#### Impact of U0126 and Trametinib administration

U0126, an inhibitor of Mek1 and Mek2 (Davies *et al.*, 2000), was employed at 5  $\mu$ M concentration, and distinctive phenotypes were recorded for up to three weeks following drug administration. Preliminary studies revealed that concentrations of >7  $\mu$ M caused colonial mortality, whereas concentrations of <1  $\mu$ M had no phenotypic impact (data not shown). In total, seven colonies at blastogenic phase "A" were submersed for 72 h in 5  $\mu$ M U0126 containing seawater, and closely monitored for up to 17 days thereafter, with parallel blastogenic phase and genet matching controls. Documentation of the phenotypic impacts of the treatment was performed (Fig. 8 A,H,K-O), and immunological and histological analyses were done on several treated genets. First impact signs were observed two days following U0126 administration, seen as significant reduction in p-Mek1 staining of primary buds (Fig. 8 B,C) and germ lineage cells staining in all modules (Fig. 8B, C). Malformed primary buds were observed as early as two days

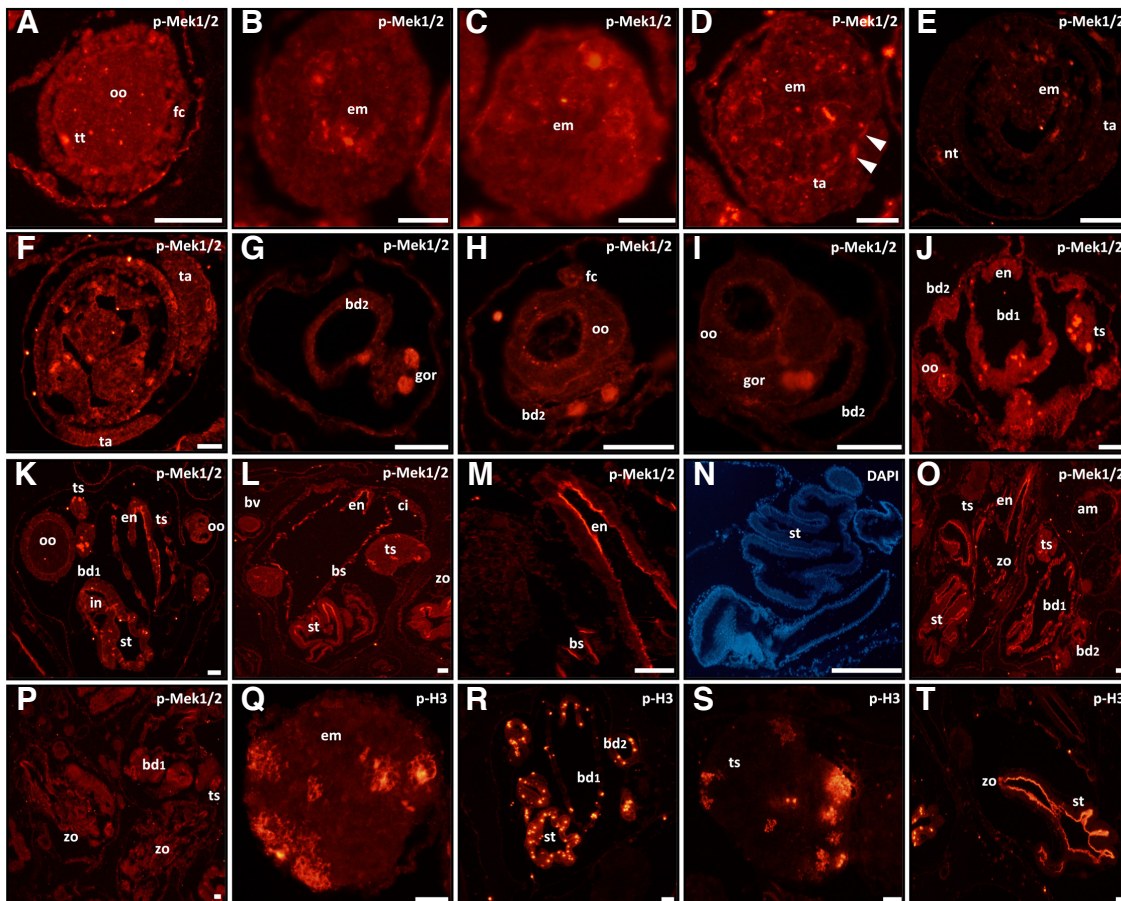


**Fig. 7. p-Mek1/2 normal expression along embryogenesis and blastogenesis.** Immunohistochemical staining with anti p-Mek1/2 antibodies (A-M, O-P), with anti p-Histone 3 antibodies (Q-T) or DAPI staining of a tissue (N). The tissues derived from control animals are: (A) egg; (B-F) embryos at various developmental phases; (G-I) secondary buds; (J-K) primary buds; (L) blastogenic phase "A" zooid; (M) blastogenic phase "A" zooidal endostyle; (N) blastogenic phase "A" zooidal digestive system; (O) blastogenic phase "C" zooid; (P) blastogenic phase "D" zooid; (Q) embryo; (R) primary and secondary bud; (S) zooidal testis; (T) blastogenic phase "C" zooid. Abbreviations: am, ampulla; bd1, primary bud; bd2, secondary bud; bs, branchial sac; bv, blood vessel; em, embryo; en, endostyle; fc, follicular cells; gor, gonad rudiment; in, intestine; nt, notochord; oo, oocyte; st, stomach; ta, tail; ts, testis; tt, test cells; tu, tunic; zo, zooid.

Bar=50 $\mu$ m

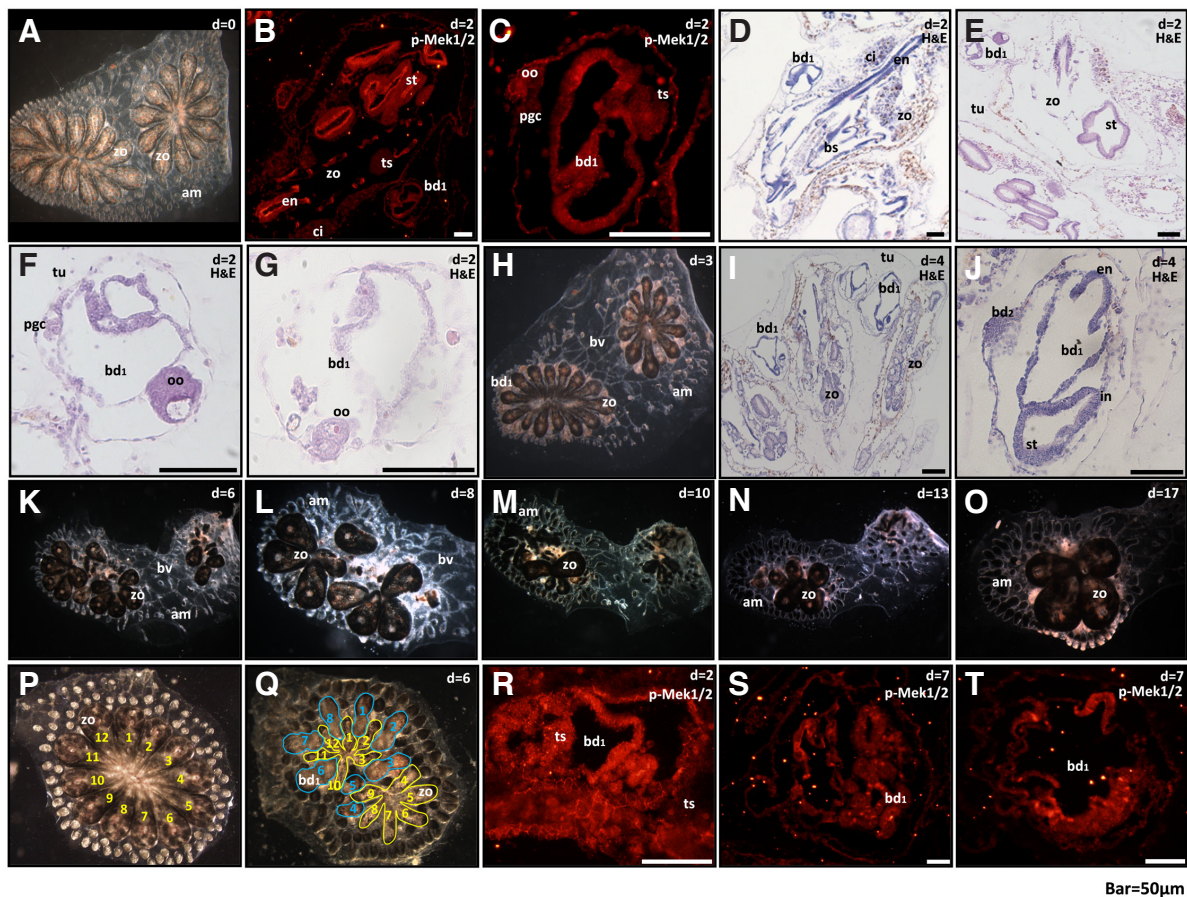


**Fig. 8. Effects of Mek1/Mek2 kinase activity inhibitors on *B. schlosseri* colonies.** U0126 effects (A-O); Trametininib effects (P-T). Gross morphologies of *B. schlosseri* colonies (A, H, K-Q), immunohistochemical staining performed with either p-Mek1/2 antibody and visualized with Cy<sup>3</sup>-conjugated antibody (B-C, R-T) or hematoxylin and eosin staining (D-G, I-J) as specified on each picture. Time after U0126 or Trametininib administration is specified, setting first treatment day as d=0. The panel includes: (A) whole colony before treatment; (B, D-E, H-I, K-O) a portion of U0126 treated colony; (C, F, G, J) U0126 treated primary buds; (P) a colony before and (Q) six days after Trametininib treatment; (R-T) primary buds after Trametininib treatment. On (P) and (Q), yellow numbers/outlines mark zooids, blue numbers/outlines mark primary buds. Abbreviations: am, ampulla; bd1, primary bud; bd2, secondary bud; bv, blood vessel; ci, cell islands; en, endostyle; H&E, hematoxylin and eosin staining; oo, oocyte; PGC, PGC-like cells; st, stomach; ts, testis; tu, tunic; zo, zooid.

following U0126 administration (Figs. 8 D-G), abreast few normal looking buds and zooids (Fig. 8D). On day 3, the two systems constituting the specific ramet studied (Fig. 8H) withdrew from each other, retracting blood vessels and ampullae, while primary buds grew rapidly. Hematoxylin and eosin staining (d=4) revealed early absorption of the zooidal internal organs (Fig. 8I) and relatively small primary buds with poorly differentiated internal organs (Fig. 8I), side by side with normal looking primary buds with secondary buds (Fig. 8J). The 'takeover' phase occurred faster than normal (cycle lasting 6 days instead of 7), as observed in stressed animals (unpublished). The result of the high number of malformed buds was a 40% decrease in zooid number after 'takeover' (the number of zooids in the newly emerged generation was reduced to 15, compared to 25 in the previous generation; Fig. 8K and Fig. 8A, respectively). Despite the decrease in number, the zooids reorganized in three colonial systems, with an additional zooid separated from the rest (Figs. 8L). Stress signs were discernible by increased pigmentation, shrinking ampullae and blood vessel dilatation. In the next blastogenic cycle, the number of zooids

further decreased to five (Fig. 8M). From this stage onwards, the surviving colonies started to recover (Fig. 8 N-O). Three colonies out of seven (43%) survived the treatment.

The specificity of the U0126 treatment was further verified by Trametininib, another inhibitor of Mek1/Mek2. Trametininib was delivered at a concentration of 0.7nM (IC<sub>50</sub> of 0.92 and 1.8 nM for Mek1 and Mek2, respectively, according to the manufacturer), for 3 days on 7 naïve colonies and impacts were compared to those of seven genet matched DMSO treated controls. Comparison of a colony before (Fig. 8P) and six days following Trametininib treatment (at phase 'D'; Fig. 8Q) revealed a 33% decrease in zooid numbers after 'takeover', since only eight normal sized primary buds developed to replace the twelve existing zooids. Immunohistochemical analysis with p-Mek1/2 antibodies showed unstained and undifferentiated primary buds two days following treatment (Fig. 8R). Seven days following treatment, p-Mek positively stained differentiated (Fig. 8S) and under-differentiated primary buds (Fig. 8T) were spotted in the same colony.

U0126 and Trametininib impacts, among them the decrease in

colony size, were probably caused by the differentiation failure of a large fraction of the primary buds, and are common to both inhibitors.

## Discussion

This study focuses on STP expression and functions during astogeny and ontogeny, using the colonial ascidian *B. schlosseri* as a model. In solitary ascidian species, STP expression and functions during ontogenic stages have been elucidated for Wnt/ $\beta$ -catenin (Niwano et al., 2009; Hudson et al., 2013), TGF- $\beta$  (Kobayashi et al., 1999; Kobayashi and Makabe, 2001; Hino et al., 2003; Kawashima et al., 2005; Christiaen et al., 2010; Nishide et al., 2012) and MAPK/ERK (Bertrand et al., 2003; Hudson et al., 2003; Nishida, 2003; Pasini et al., 2006; Chambon et al., 2007; Sakabe et al., 2006) pathways alone, or in combination with other STPs (Hudson et al., 2007; Lemaire, 2009; Pasini et al., 2012; Sasakura et al., 2012; Squarzone et al., 2011). This has not been extensively studied in colonial species where astogenic and ontogenic pathways are developing side by side and in concert.

Botryllid ascidians are colonial marine chordates with a remarkable astogeny, manifested by consecutive and serial blastogenic cycles. Both astogeny and ontogeny form similar bodily structures (Manni and Burighel, 2006), including axial polarity and colonial patterning, all adhering to the rules of stem cell proliferation and differentiation. Therefore, it is assumed that basic evolutionary traits, like STPs, could be shared between embryogenesis and astogeny (such as blastogenesis; Gasparini et al., 2011), as well as with major regeneration routes (Rinkevich et al., 2008), taking also into account that modulation of Wnt/ $\beta$ -catenin, MAPK/Erk and TGF- $\beta$  pathways enhances somatic cell reprogramming in ways that are still poorly understood (Sanges and Cosma, 2010). Colonial ascidians, with their recurring blastogenic cycles and their close relationship with the vertebrates, are thus excellent models for studying these relationships. However, while studies (e.g., Bertrill, 1941a,b; Izzard, 1973; Sabbadin et al., 1975; Lauzon et al., 2002) have already described major routes in the botryllid ascidian astogeny, knowledge regarding the molecular programs in colonial ascidians is limited. Tiozzo et al., (2005) studied the expression of pitx (pituitary homeobox gene) and Gasparini et al., (2011) studied the outcomes for the expression of a Musashi-like gene in blastogenesis and embryogenesis. pmERK (MAPK pathway) and pm $\beta$ -CTN ( $\beta$ -catenin orthologue) were shown to be strongly induced in *Polyandrocarpa misakiensis* trans-differentiating buds (Kawamura et al., 2013) following RA treatment. RA also regulated secondary axis formation (Hara et al., 1992) and triggered an epithelium trans-differentiation of the gut in regenerating animals, as they might do in buds (Kaneko et al., 2010).

Here we studied Wnt/ $\beta$ -catenin, TGF- $\beta$  and MAPK pathways by elucidating the participation of a focal gene from each of the above STPs ( $\beta$ -Catenin for the Wnt pathway, Smad2 and Smad1/5/8 for the TGF- $\beta$  pathway, and Mek1/2 for MAPK/ERK pathway), investigating functionality in astogeny and ontogeny through the administration of specific inhibitors/activators. Results further reveal that the three STPs are co-expressed (but not necessarily co-localized; Fig. 9) during astogeny and ontogeny, with STP-specific spatiotemporal patterns.

$\beta$ -catenin structural and signaling functions (Valenta et al., 2012) are mediated at different cellular compartments, the sub-membrane and the nucleus. In *B. schlosseri*, high nuclear  $\beta$ -catenin expressions

are detected in the vegetal pole of early staged embryos, similar to solitary tunicates (Hudson et al., 2013), and in endostyles of late embryos, a location not been previously described. Submembranal  $\beta$ -catenin expressions appear in differentiating embryos where the majority of  $\beta$ -catenin resides, a property shared with buds and zooids of blastogenic phases "A" to "C". In buds of all blastogenic phases, we could not observe strong nuclear  $\beta$ -catenin accumulation, but rather low expressions distributed equally in cytoplasm and nuclei. The endostyle zone 4 tissues expressed the highest  $\beta$ -catenin levels (in both nuclei and cytoplasm) at blastogenic phases "A", "B" and early "C", and became dramatically down-expressed at advanced blastogenic phase "C", prior to the onset of the 'take over' process. Either knockdown (Chang et al., 2013) or overexpression (Kim et al., 2000) of  $\beta$ -catenin may induce apoptosis. In this study, though agonist treatment in blastogenic phase "A" treated colonies induced the premature destruction of internal organs in zooids, it did not accelerate the blastogenic cycle, but instead extended it. Antagonist administration, in contrast, accelerated the blastogenic

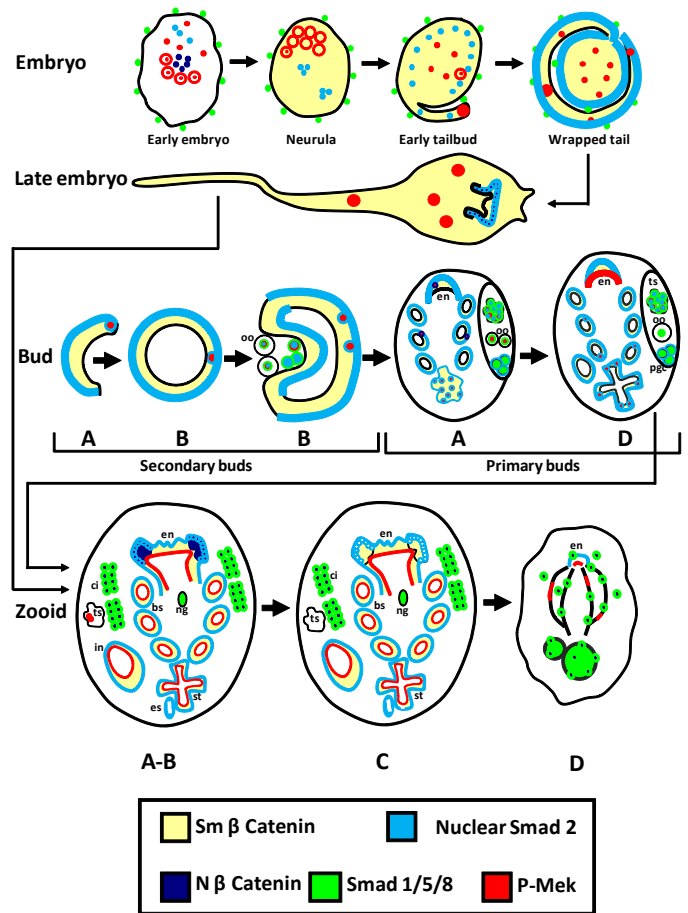


**Fig. 9. Graphical summary.** Summary of p-Smad1/5/8, p-Smad2,  $\beta$ -Catenin and p-Mek1/2 co-expressions in astogeny (buds and zooids along blastogenic phases "A" to "D"; sensu Mukai and Watanabe, 1976) and ontogeny, and in the corresponding stages of gonadogenesis and embryogenesis. Arrows refer to the weekly concurrent progress in the three developmental phenomena during one blastogenic cycle. Sm  $\beta$  catenin and N  $\beta$  catenin refer to submembranal and nuclear  $\beta$  catenin, respectively. Abbreviations: ci, cell islands; en, endostyle; es, esophagus; in, intestine; ng, neural gland; oo, oocyte; PGC, PGC-like cells; st, stomach; ts, testis.

cycle. However, treating late blastogenic “C” colonies (when buds are almost completely differentiated) with Wnt agonist did not change the duration of the existing blastogenic cycle, implying that  $\beta$ -catenin was not the primary pacemaker of the blastogenic cycle. As in other models, the responses to the  $\beta$ -catenin agonist or antagonist depend on responder characteristics; embryos responded to either agonist or inhibitor treatments with an arrest of differentiation followed by death, while buds responded with malformed differentiation. In the zooids, Wnt agonist caused internal organ apoptosis concurrent with macrophage-like cells activation and the migration of these cells out of the resident cell islands to various zooidal tissues, all revealed by an increase in the content of the macrophage  $\beta$ -catenin. As for the germ lineage,  $\beta$ -catenin was expressed in stem or early differentiating cell types such as PGC-like or gonial cells and in the follicular layers of the oocytes.

TGF- $\beta$ , Activin and Nodal signals are mediated via p-Smad2. Nuclear p-Smad2 expression patterns in *B. schlosseri* gastrula and tail-bud embryos are differentially expressed with regards to site/time (Fig. 9). In wrapped-tail embryos, buds and zooids, p-Smad2 nuclear expression is ubiquitous in almost all cell types, with fluctuating staining strength in various tissues, of which the most prominent staining is in the zooidal esophagus, in both the nucleus and the cytoplasm. Inhibition of TGF- $\beta$ /Activin pathways reduced p-Smad2 staining, also resulting in malformation in the primary buds along the A/P axis: degenerated/malformed tissue at the anterior part of the buds (endostyle, branchial sac), with healthy looking tissues at the posterior part (stomach). The L/R axis was also affected as the stomach and intestine shifted to the right following the formation of large cavities. On the colonial level, system unit formation was lost and replaced by a chaotic distribution of the zooids, resembling changes that were induced in *B. schlosseri* colonies by retinoic acid treatment (Rosner *et al.*, 2013).

BMP signals are transmitted via phosphorylation of Smad1/5/8. The p-Smad1/5/8 expression results of this study suggest that BMP functions in germ cell homeostasis and differentiation and in zooid apoptosis. Negative (or very low) p-Smad1/5/8 staining was observed in buds and embryos. The weak p-Smad1/5/8 staining in embryos contradicted the well documented BMP input to the heart and nervous systems specifications, described in other ascidians (Pasini *et al.*, 2006; Christiaen *et al.*, 2010). Therefore, functions in the *B. schlosseri* BMP pathways should be further studied.

p-Mek is an activated intermediate molecule of the MAPK/ERK pathway. p-Mek molecules phosphorylate Erk, which are then translocated to the nucleus, and to a lesser extent to the cell periphery. Thereafter, p-Mek molecules are rapidly exported out of the nucleus (Jaaro *et al.*, 1997). ELISA analysis showed fluctuation in p-Mek quantity as embryos differentiated, while the quantity of p-Mek continuously increased as the buds matured. Immunohistochemical analyses indicated that p-Mek is distributed in three different subcellular compartments, nuclear, cytoplasmic and sub-membrane, all detected in buds and embryos (Fig. 9). The *B. schlosseri* embryonic p-Mek staining pattern resembled that of dp-Erk in *C. intestinalis* embryos, primarily in early and mid-tail bud stages (Pasini *et al.*, 2012). Nuclear p-Mek expressions were the highest in differentiating primary buds, primarily in the gut rudiment, the differentiating digestive system and the testes. The dispersed expression pattern of p-Mek in buds resembled that of p-H3, a proliferation marker, which suggests that in buds the MAPK pathway regulates proliferation, as reported in other organisms (Liu

*et al.*, 2004). Colonies treated with the Mek inhibitors U0126 or with Trametinib contained poorly differentiated/malformed primary buds, which also indicates an additional function in buds tissue specification, as described in *C. intestinalis* embryos (Hudson *et al.*, 2003; Nishida, 2003). Conversely, the nature and function of the continuous apical sided p-Mek staining in fully differentiated buds (blastogenic phase “D”) and in adult zooids (where most of the tissues have low proliferation rate; Kawamura *et al.*, 2008) is not understood. A pro-apoptotic role during ascidian larval metamorphosis is also attributed to this pathway (Chambon *et al.*, 2007). Since U0126 or the Trametinib block of p-Mek1/2 kinase activity did not significantly affect the blastogenic cycle duration or the ‘takeover’ process, we cannot report a similar pro-apoptotic function of Erk during astogeny.

While we have documented that the same molecular machinery is used in astogeny and ontogeny, astogenic development is not an ontogenic replicate, and provides major changes, as illustrated in Fig. 9. Early buds, in contrast to early embryos, do not form nuclear  $\beta$ -catenin-positive and negative domains in order to specify the three germ layers; nuclear Smad2 expressions are detected in all the soma cells of early buds, while expressions in early embryos are limited to only a few cells; also, the function of the nuclear Smad1/5/8 in test cells during embryogenesis is unclear, since it is not detected during bud differentiation. These major differences delineate a divergence between embryonic and bud cells, although both developmental processes are capable of forming an identical individual, the functional zooid.

## Materials and Methods

### Animals

The colonies of *B. schlosseri* used in this study were collected from shallow waters along the Israeli Mediterranean coast and from Monterey in CA, USA. In the laboratory, the animals were maintained on 5x7.5 cm glass slides, cultured in 17 l tanks in a standing seawater system at 20°C, as described by Rinkevich and Shapira (1998).

### Antibodies

Primary antibodies: Rabbit anti Phospho-Smad2 (Ser465/467) #3101 Cell Signaling Technology (dilution 1:200); Phospho-Smad1 (Ser463/465)/Smad5 (Ser463/465)/Smad8 (Ser426/428) #9511 Cell Signaling Technology (dilution 1:100); Rabbit anti  $\beta$ -catenin (H-102) sc-7199 Santa Cruz; Biotechnology (dilution 1:200); Rabbit anti Phospho-Mek1/2 (Ser217/221) #9121 Cell Signaling Technology (dilution 1:100); Rabbit polyclonal p-Histone H3 (Ser 10)-R: sc-8656-R Santa Cruz 1:400; Poly clonal Rabbit anti BS-PL10 (Rosner *et al.*, 2006, dilution 1:4000); Poly clonal Rabbit anti BS-cadherin (Rosner *et al.*, 2007, dilution 1:4000).

Secondary antibodies: Cy<sup>TM</sup>3-conjugated AffiniPure Goat Anti-Rabbit IgG (H+L) Amax-550; Emax 570 (Cat. No. 111-165-003; Jackson ImmunoResearch laboratories, USA). DyLight<sup>TM</sup> 488-conjugated affinity pure Fab Fragment Goat anti-Rabbit IgG (H<sub>p</sub>L) Amax-493; Emax 518 (Cat. no. 111-487-003; Jackson ImmunoResearch laboratories). Alkaline Phosphatase-conjugated goat anti-Rabbit Jackson ImmunoResearch (Cat. No. 111-055-144; West Grove, PA USA), was used at dilution of 1:10,000. Slides are mounted in Fluoromount medium (fluorescent antibodies; Sigma Cat. No. F 4680) or Hydromount (for AP conjugated antibodies; Partial Diagnostics, Atlanta, Georgia, USA).

### DAPI staining

DAPI (Cat. No. D9564, sigma, USA; absorption peak: 350 nm; emission peak: 460 nm) stock solution was diluted to 300 nM in PBS. 300  $\mu$ L of this diluted DAPI solution was added to each slide. After a 5 min.

incubation, the slides were washed several times in PBS and mounted in Fluoromount medium.

#### Immunoblots

Total proteins were extracted as described by Rosner *et al.*, (2013). Tissues were boiled for 3 min before being loaded on SDS-PAGE. The Western blotting analysis was adapted for Odyssey detection as recommended ([http://biosupport.licor.com/docs/Western\\_Blot\\_Analysis\\_11488.pdf](http://biosupport.licor.com/docs/Western_Blot_Analysis_11488.pdf)), with Anti-Rabbit IgGIRDye 800CW 611-131-002S (Rockland, PA, USA) as a secondary antibody.

#### ELISA

Wells of ELISA plate (F96 Maxisorp, immuno plate 442404, Nunc, Denmark) were coated with *B. schlosseri* extracts from different tissues (20 µg/ml diluted in 0.1M carbonate buffer pH 9.8), incubated over night at 4°C, fixed with 10% formaldehyde for 10 min at 4°C, and then washed 4x5 min each, with PBS containing 0.05% Tween 20 (PBS-T). Wells were post coated with 4% bovine serum albumin in PBS-T, incubated over night at 4°C and then washed. The primary antibodies were each added to the wells and incubated for 2 h at 37°C, then washed. Goat anti rabbit IgG conjugated to alkaline phosphatase (No 111 055 144 Jackson Research Laboratories, USA) was added and incubated for 1 h at 37°C, then washed. A substrate to alkaline phosphatase p-nitrophenyl phosphate (pNPP S0942) was added (1 mg/ml) and incubated for 2 h at 37°C, followed by an overnight incubation at 4°C. The optical density (OD) was determined using the GLOMAX Multi+ Detection System (model E9032, Promega Corporation Instrument, USA) at 405 nm. Each ELISA result was expressed as a ratio between the mean absorbance by the specific antibody (P) and the mean absorbance in negative background (N) (Lapidot, 1995, 2003).

#### Histology and immunohistochemistry

Animals were fixed in Bouin's solution (Humason, 1962) for 1-2 h, dehydrated in a series of graded ethanol (70-100%) and 100% butanol and embedded in paraffin wax (paraplast). Cross serial sections (5 µm) were obtained by hand-operated microtome (Leica, Nussloch, Germany) stained with hematoxylin and eosin for general morphology.

Immunohistochemistry was performed according to Rosner *et al.*, (2009). Retrieval was performed in a Tris-EDTA Buffer (pH 9.0). When goat anti-rabbit AP was used as a secondary antibody, the staining was performed in NBT/BCIP solution. The stained sections were mounted either onto Fluoromount for fluorescent antibody (Cat. No. F4680, Sigma) or onto Hydromount™ mounting medium (Cat. No. HS-106, Patorial diagnostics, Atlanta, GA, USA).

#### Specific inhibitors/activator

Six inhibitors/activators, specific to one of the studied STPs (Wnt/β-catenin; TGF-β, MAPK/ERK) were employed on whole animal settings in 200 ml glass vessels. For the Wnt/β-catenin pathway we studied the effects of an agonist and of an antagonist: (1) the Wnt agonist, 2-Amino-4-(3,4-(methylenedioxy) benzylamino)-6-(3-methoxyphenyl) pyrimidine (Calbiochem; Cat. No. 681665; dissolved in DMSO, dimethyl sulfoxide), is a cell-permeable, potent activator of Wnt signaling that does not inhibit the activity of GSK-3β, which has been shown to mimic the effects of Wnt and induce β-catenin and T-cell fate-dependent transcriptional activity (Liu *et al.*, 2005); (2) The Wnt antagonist XAV939 (IC<sub>50</sub>=4 nM; CAS 284028-89-3; Cayman Chemicals, MI, USA; soluble in DMSO) antagonizes Wnt signaling via stimulation of β-catenin degradation and stabilization of axin. For the TGF-β pathway, we used two inhibitors: (1) SB-431542 (cat. no S4317, Sigma-Aldrich; soluble in DMSO), a potent inhibitor of the TGF-β superfamily type I activin receptor-like kinase (ALK), a receptor that has no effect on BMP signaling and therefore does not inhibit Smad1/5/8 (Inman *et al.*, 2002); (2) LY2157299 an inhibitor of the TGF-β receptor type I kinase (CAS No. 700874-72-2, Cayman Chemical MI, USA). For inhibiting the MAPK/ERK pathway, we used the two Mek inhibitors: (1) U0126 (Cat. No. V112, promega, Wisconsin; soluble in DMSO), 1,4-Diamino-2,3-dicyano-1,4-

bis-(o-aminophenylmercapto) butadiene ethanolate, an inhibitor of both Mek1 and Mek2 (Favata *et al.*, 1998); (2) Trametinib (trade name Mekinist; CAS. No. 87100-17-3, Santa Cruz Biotechnology, USA soluble in DMSO). Trametinib is also an inhibitor of Mek1/Mek2 activity.

Three colonies were subjected overnight to 1000 µM of H<sub>2</sub>O<sub>2</sub> (Cat. No. H1009, Sigma, USA), while three other colonies were subjected to 25 nM of retinoic acid (Cat. No. R2625; Sigma, USA) for two days as described by Rosner *et al.*, (2007, 2013, respectively). Control colonies were subjected to the suitable solvent concentrations (DMSO) in similar 200 ml vessels. Experiments were run for 24, 48, or 72 h, after which the treated *B. schlosseri* colonies were returned to their regular 17 L seawater aquaria.

#### Acknowledgements

This study was supported by grants from the Israel Academy of Science (1342/08 and 68/10).

#### References

- BALLARIN L, BURIGHEL P and CIMA F (2008). A tale of death and life: natural apoptosis in the colonial ascidian *Botryllus schlosseri* (Urochordata, Ascidiacea). *Curr Pharm Des* 14: 138-147.
- BERRILL N J (1941a). The development of bud in *Botryllus*. *Biol Bull* 80: 169-184.
- BERRILL N J (1941b). Size and morphogenesis in the bud of *Botryllus*. *Biol Bull* 80: 185-193.
- BERRILL N J (1950). The Tunicata with an account of the British species. Ray Society, London.
- BERTRAND V, HUDSON C, CAILLOLD, POPOVICI C and LEMAIRE P (2003). Neural tissue in ascidian embryos is induced by FGF9/16/20, acting via a combination of maternal GATA and Ets transcription factors. *Cell* 115: 615-627.
- CHAMBON J P, NAKAYAMAA, TAKAMURAK, MCDUGALLA and SATOH N (2007). ERK and JNK-signaling regulate gene networks that stimulate metamorphosis and apoptosis in tail tissues of ascidian tadpoles. *Development* 134: 1203-1219.
- CHANGH W, LEE Y S, NAM H Y, HAN M W, KIM H J, MOON S Y, JEON H, PARK J J, CAREY T E, CHANG S E, KIM S W and KIM S Y (2013). Knockdown of β-catenin controls both apoptotic and autophagic cell death through LKB1/AMPK signaling in head and neck squamous cell carcinoma cell lines. *Cell Signal* 25: 839-847.
- CIMA F, BALLARIN L (2009). Apoptosis and pattern of Bcl-2 and Bax expression in the alimentary tract during the colonial blastogenetic cycle of *Botryllus schlosseri* (Urochordata, Ascidiacea). *Italian J Zool* 76: 28-42.
- CHRISTIAEN L, STOLFI A and LEVINE M (2010). BMP signaling coordinates gene expression and cell migration during precardiac mesoderm development. *Dev Biol* 340: 179-187.
- DAVIES S P, REDDY H, CAIVANOM and COHEN P (2000). Specificity and mechanism of action of some commonly used protein kinase inhibitors. *Biochem J* 351: 95-105.
- DELSUC F, BRINKMANN H, CHOURROUT D and PHILIPPE H, (2006). Tunicates and not cephalochordates are the closest living relatives of vertebrates. *Nature* 439: 965-968.
- FAVATAM, HORIUCHI K Y, MANOS E J, DAULERIO A J, STRADLEY D A, FEESER W S, VAN DYK D E, PITTS W J, EARL R A, HOBBS F, COPELAND R A, MAGOLDA R L, SCHERLE P A and TRZASKOS J M (1998). Identification of a novel inhibitor of mitogen-activated protein kinase kinase. *J Biol Chem* 273: 18623-18632.
- FRANCHI N, SCHIAVON F, BETTI M, CANESI L and BALLARIN L (2013). Insight on signal transduction pathways involved in phagocytosis in the colonial ascidian *Botryllus schlosseri*. *J Invertebr Pathol* 112: 260-266.
- GASPARINI F, SHIMELD S M, RUFFONI E, BURIGHEL P and MANNI L (2011). Expression of a Musashi-like gene in sexual and asexual development of the colonial chordate *Botryllus schlosseri* and phylogenetic analysis of the protein group. *J Exp Zool (Mol Dev Evol)* 316: 562-573.
- HARAK, FUJIWARAS and KAWAMURAK (1992). Retinoic Acid can induce a Secondary Axis in Developing Buds of a Colonial Ascidian, *Polyandrocarpa misakiensis*. *Dev Growth Differ* 34: 437-445.
- HINO K, SATOU Y, YAGI K and SATOH N (2003). A genome wide survey of developmentally related genes in *Ciona intestinalis*: VI, Genes for Wnt, TGFβ, Hedgehog and JAK/STAT signaling pathways. *Dev Genes Evol* 13: 264-272.
- HUDSON C, KAWAI N, NEGISHIT and YASUOH (2013). β-Catenin-driven binary fate

- specification segregates germ layers in ascidian embryos. *Curr Biol* 23: 491-495.
- HUDSON C, LOTITO S and YASUO H. (2007). Sequential and combinatorial inputs from Nodal, Delta2/Notch and FGF/MEK/ERK signalling pathways establish a grid-like organisation of distinct cell identities in the ascidian neural plate. *Development* 134: 3527-3537.
- HUDSON C, DARRAS S, CAILLOL D, YASUO H and LEMAIRE P (2003). A conserved role for the MEK signalling pathway in neural tissue specification and posteriorisation in the invertebrate chordate, the ascidian *Ciona intestinalis*. *Development* 130: 147-159.
- HUGHES R N (2005). Lessons in modularity: the evolutionary ecology of colonial invertebrates. *Sci Mar* 69: 69-179.
- HUMASON G L (1962). Fixation and specific staining methods. In: Animal Tissue Technique (Eds. R. E. D. Kennedy and R. B. Park). W. H. Freeman and Company, San Francisco and London, pp. 14-163.
- IMAI K, TAKADA N, SATOH N and SATOU Y (2000).  $\beta$ -catenin mediates the specification of endoderm cells in ascidian embryos. *Development* 127: 3009-3020.
- INMAN G, NICOLAS F, CALLAHAN J, HARLING J, GASTER L, REITH A, LAPING N and HILL C (2002). SB-431542 is a potent and specific inhibitor of transforming growth factor- $\beta$  superfamily Type I activin receptor-like kinase (ALK) receptors ALK4, ALK5, and ALK7. *Mol Pharmacol* 62: 65-74.
- IZZARD C S (1973). Development of polarity and bilateral asymmetry in the palleal bud of *Botryllus schlosseri* (Pallas). *J Morphol* 139: 1-25.
- JAARO H, RUBINFELD H, HANOCH T and SEGER R (1997). Nuclear translocation of mitogen-activated protein kinase kinase (MEK1) in response to mitogenic stimulation. *Proc Natl Acad Sci USA* 94: 3742-3747.
- KANEKON, KATSUYAMA Y, KAWAMURAK, and FUJIWARA S (2010). Regeneration of the gut requires retinoic acid in the budding ascidian *Polyandrocarpa misakiensis*. *Dev Growth Differ* 52: 457-468.
- KAWAMURA K, SHIOHARA M, KANDA M and FUJIWARA S (2013). Retinoid X receptor-mediated transdifferentiation cascade in budding tunicates. *Dev Biol* 384: 343-355.
- KAWAMURA K, TACHIBANA M, SUNANAGA T (2008). Cell proliferation dynamics of somatic and germline tissues during zooidal life span in the colonial tunicate *Botryllus primigenus*. *Dev Dyn* 237: 1812-1825.
- KAWASHIMA T, SATOU Y, MURAKAMI S D, and SATOH N (2005). Dynamic changes in developmental gene expression in the basal chordate *Ciona intestinalis*. *Dev Growth Differ* 47: 187-199.
- KIM K, PANG K M, EVANS M, and HAY E D (2000). Overexpression of beta-catenin induces apoptosis independent of its transactivation function with LEF-1 or the involvement of major G1 cell cycle regulators. *Mol Biol Cell* 11: 3509-3523.
- KOBAYASHI A, MAKABE K W (2001). Expression patterns of Smad family members during embryogenesis of the ascidian *Halocynthia roretzi*. *Zool Sci* 18: 833-842.
- KOBAYASHI A, SASAKURA Y, OGASAWARA M and MAKABE K W (1999). A maternal RNA encoding smad1/5 is segregated to animal blastomeres during ascidian development. *Dev Growth Differ* 41: 419-427.
- KOMIYA Y, HABAS R (2008). Wnt signal transduction pathways. *Organogenesis* 4: 68-75.
- KOURAKIS M J, SMITH WC (2007). A conserved role for FGF signaling in chordate otic/atrial placode formation. *Dev Biol* 312: 245-257.
- KUECKEN M, RINKEVICH B, SHAISH L and DEUTSCH A (2011). Nutritional resources as positional information for morphogenesis in the stony coral *Stylophora pistillata*. *J Theor Biol* 275: 70-77.
- LAPIDOT Z, SIMAN-TOV R and NAOT Y (1995). Monoclonal antibody that inhibit mitogen activity of mycoplasma pulmonis. *Infect Immun* 63: 34-141.
- LAPIDOT Z, PAZ G, and RINKEVICH B (2003). Monoclonal antibody specific to urochordate *Botryllus schlosseri* pyloric gland. *Mar Biotechnol* 5: 88-394.
- LAUZON R J, ISHIZUKA K. J, and WEISSMAN I L (2002). Cyclical generation and degeneration of organs in a colonial urochordate involves crosstalk between old and new: a model for development and regeneration. *Dev Biol* 249: 333-348.
- LEMAIRE P (2009). Unfolding a chordate developmental program, one cell at a time: invariant cell lineages, short-range inductions and evolutionary plasticity in ascidians. *Dev Biol* 332: 48-60.
- LIU J, WU X, MITCHELL B, KINTNER C, DING S and SCHULTZ, P G (2005). A small-molecule agonist of the Wnt signaling pathway. *Angew Chem Int Ed Engl* 44: 1987-1990.
- LIU X, YAN S, ZHOU T, TERADA Y and ERIKSON R L (2004). The MAP kinase pathway is required for entry into mitosis and cell survival. *Oncogene* 23: 763-776.
- MANNI L, BURIGHEL P (2006). Common and divergent pathways in alternative developmental processes of ascidians. *Bioessays* 28: 902-912.
- MANNI L, ZANIOLO G, CIMA F, BURIGHEL P and BALLARIN L (2007). *Botryllus schlosseri*: a model ascidian for the study of asexual reproduction. *Dev Dyn* 236: 335-352.
- MILKMAN R (1967). Genetic and developmental studies on *Botryllus schlosseri*. *Biol Bull (Woods Hole)* 132: 229-243.
- MUKAI H, WATANABE H (1976). Studies on the formation of germ cells in a compound ascidian *Botryllus primigenus*. *Oka J Morphol* 148: 337-361.
- NISHIDA H (2003). Spatio-temporal pattern of MAP kinase activation in embryos of the ascidian *Halocynthia roretzi*. *Dev Growth Differ* 45: 27-37.
- NISHIDE K, MUGITANI M, KUMANO G, and NISHIDA H (2012). Neurula rotation determines left-right asymmetry in ascidian tadpole larvae. *Development* 139: 1467-1475.
- NIWANO T, TAKATORI N, KUMANO G and NISHIDA H (2009). Wnt5 is required for notochord cell intercalation in the ascidian *Halocynthia roretzi*. *Biol Cell* 101: 645-659.
- ODA H (2012). Evolution of the Cadherin-Catenin Complex. In *Adherens Junctions: From Molecular Mechanisms to Tissue* (Ed T Harris). Springer Science+Business Media Dordrecht, pp. 9-35.
- PACHUT J F, CUFFEY R F and ANSTEY R L (1991). The concepts of astogeny and ontogeny in stenolaemate bryozoans, and their illustration in colonies of *Tubulipora carbonaria* from the lower Permian of Kansas. *J Paleont* 65: 213-233.
- PASINI A, AMIEL A, ROTHBÄCHER U, ROURE A, LEMAIRE P and DARRAS, S. (2006). Formation of the ascidian epidermal sensory neurons: Insights into the origin of the chordate peripheral nervous system. *PLoS Biol* 4: e225.
- PASINI A, MANENTI R, ROTHBÄCHER U and LEMAIRE P (2012). Antagonizing retinoic acid and FGF/MAPK pathways control posterior body patterning in the invertebrate chordate *Ciona intestinalis*. *PLoS One* 7: e46193.
- RINKEVICH B (2002). The branching coral *Stylophora pistillata*: The contribution of genetics in shaping colony landscape. *Isr J Zool* 48: 71-82.
- RINKEVICH B, SHAPIRA M (1998). An improved diet for inland broodstock and the establishment of an inbred line form *Botryllus schlosseri*, a colonial sea squirt (Asciacea). *Aquat Living Resour* 11: 163-171.
- RINKEVICH Y, RINKEVICH B and RESHEF R (2008). Cell signaling and transcription factor genes expressed during whole body regeneration in a colonial chordate. *BMC Dev Biol* 8: 100.
- ROSNER A, MOISEEVA E, RABINOWITZ C and RINKEVICH B (2013). Germ lineage properties in the urochordate *Botryllus schlosseri* - From markers to temporal niches. *Dev Biol* 384: 356-374.
- ROSNER A, MOISEEVA E, RINKEVICH Y, LAPIDOT Z and RINKEVICH B (2009). Vasa and the germ line lineage in a colonial urochordate. *Dev Biol* 331: 113-128.
- ROSNER A, PAZ G and RINKEVICH B (2006). Divergent roles of the DEAD-box protein BS-PL10, the urochordate homologue of human DDX3 and DDX3Y proteins, in colony astogeny and ontogeny. *Dev Dyn* 235: 1508-1521.
- ROSNER A, RABINOWITZ C, MOISEEVA E, VOSKOBOYNIK A and RINKEVICH B (2007). BS-cadherin in the colonial urochordate *Botryllus schlosseri*: one protein, many functions. *Dev Biol* 304: 687-700.
- SABBADIN A, BURIGHEL P and ZANIOLO, G. (1992). Some aspects of reproduction in ascidians. In: Sex and Evolution (Ed. R. Dallai). Selected Symposia and Monographs U.Z.I. 6. Mucchi, Modena, pp. 103-115.
- SABBADIN A, ZANIOLO G and MAJONE F (1975). Determination of polarity and bilateral asymmetry in palleal and vascular buds of the ascidian *Botryllus schlosseri*. *Dev Biol* 46: 79-87.
- SAKABE E, TANAKA N, SHIMOZONO N, GOJOBORI T and FUJIWARA S (2006). Effects of U0126 and fibroblast growth factor on gene expression profile in *Ciona intestinalis* embryos as revealed by microarray analysis. *Dev Growth Differ* 48: 391-400.
- SÁNCHEZ JA, LASKER H R (2003). Patterns of morphological integration in marine modular organisms: supra-module organization in branching octocoral colonies. *Proc R Soc Lond B* 270: 2039-2044.
- SANGES D, COSMA M P (2010). Reprogramming cell fate to pluripotency: the decision-making signalling pathways. *Int J Dev Biol* 54: 575-1587.

- SASAKURA Y, KANDA M, IKEDA T, HORIE T, KAWAI N, OGURA Y, YOSHIDA R, HOZUMI A, SATOH N and FUJIWARA S (2012). Retinoic acid-driven Hox1 is required in the epidermis for forming the otic/atrial placodes during ascidian metamorphosis. *Development* 139: 2156-2160.
- SHAISH L, ABELSON A, and RINKEVICH B (2007). How plastic can phenotypic plasticity be? The branching coral *Stylophora pistillata* as a model system. *PLoS One* 2: e644.
- SQUARZONI P, PARVEEN F, ZANETTI L, RISTORATORE F and SPAGNUOLO A (2011). FGF/MAPK/Ets signaling renders pigment cell precursors competent to respond to Wnt signal by directly controlling *Ci-Tcf* transcription. *Development* 138: 1421-1432.
- STEINHUSEN U, BADOCK V, BAUER A, BEHRENS J, WITTMAN-LIEBOLD B, DÖRKEN B and BOMMERT K (2000). Apoptosis-induced cleavage of beta-catenin by caspase-3 results in proteolytic fragments with reduced transactivation potential. *J Biol Chem* 275: 16345-16353.
- TIOZZO S, CHRISTIAEN L C, DEYTS C, MANNI L, JOLY J-S and BURIGHEL P (2005). Embryonic versus blastogenetic development in the compound ascidian *Botryllus schlosseri*: insights from *Pitx* expression patterns. *Dev Dyn* 232: 468-478.
- VALENTA T, HAUSMANN G and BASLER K (2012). The many faces and functions of  $\beta$ -catenin. *EMBO J* 31: 2714-2736.
- VOSKOBOYNIK A, NEFF N F, SAHOO D, NEWMAN A M, PUSHKAREV D, KOH W, PASSARELLI B, FAN H C, MANTALAS G L, PALMER K J, ISHIZUKA K J, GISSI C, GRIGGIO F, BEN-SHLOMO R, COREYD M, PENLAND L, WHITE R A, WEISSMAN I L and QUAKE S R (2013). The genome sequence of the colonial chordate, *Botryllus schlosseri*. *Elife* 2: e00569.
- VOSKOBOYNIK A, SIMON-BLECHER N, SOEN Y, RINKEVICH B, DE TOMASO A W, ISHIZUKA K J, and WEISSMAN I L (2007). Striving for normality: Whole body regeneration through a series of abnormal zooidal generations. *FASEB J* 21: 1335-1344.

**Further Related Reading, published previously in the *Int. J. Dev. Biol.***

**Germline stem cells and sex determination in *Hydra***

Chiemi Nishimiya-Fujisawa and Satoru Kobayashi

*Int. J. Dev. Biol.* (2012) 56: 499-508

<http://dx.doi.org/10.1387/ijdb.123509cf>

**Evolution of angiogenesis**

Ramón Muñoz-Chápuli

*Int. J. Dev. Biol.* (2011) 55: 345-351

<http://dx.doi.org/10.1387/ijdb.103212rm>

**Could modifications of signalling pathways activated after ICSI induce a potential risk of epigenetic defects?**

Brigitte Ciapa and Christophe Arnoult

*Int. J. Dev. Biol.* (2011) 55: 143-152

<http://dx.doi.org/10.1387/ijdb.103122bc>

**Hematopoietic stem cell emergence in the conceptus and the role of Runx1**

Gemma Swiers, Marella de Bruijn and Nancy A. Speck

*Int. J. Dev. Biol.* (2010) 54: 1151-1163

<http://dx.doi.org/10.1387/ijdb.103106gs>

**Roles of Src family kinase signaling during fertilization and the first cell cycle in the marine protostome worm *Cerebratulus***

Stephen A. Stricker, David J. Carroll and Wai L. Tsui

*Int. J. Dev. Biol.* (2010) 54: 787-793

<http://dx.doi.org/10.1387/ijdb.092918ss>

**Expression of prohormone convertase 2 and the generation of neuropeptides in the developing nervous system of the gastropod *Haliothis***

Scott F. Cummins, Patrick S. York, Peter H. Hanna, Bernard M. Degnan and Roger P. Croll

*Int. J. Dev. Biol.* (2009) 53: 1081-1088

<http://dx.doi.org/10.1387/ijdb.082791sc>

**Generation of a reporter-null allele of *Ppap2b/Lpp3* and its expression during embryogenesis**

Diana Escalante-Alcalde, Sara L. Morales and Colin L. Stewart

*Int. J. Dev. Biol.* (2009) 53: 139-147

<http://dx.doi.org/10.1387/ijdb.082745de>

5 yr ISI Impact Factor (2013) = 2.879

